A millennium of arable land use – the long-term impact of water and tillage erosion on landscape-scale carbon dynamics

Lena Katharina Öttl[1], Florian Wilken[1], Anna Juřicová[2,3], Pedro V. G. Batista[1], and Peter Fiener[1]

[1]Institute of Geography, University of Augsburg, Augsburg, Germany
[2]Department of Physical Geography and Geoecology, Charles University, Prague, Czech Republic
[3]Remote Sensing and Pedometrics Laboratory, Soil Survey, Research Institute for Soil and Water Conservation, Prague, Czech Republic

Correspondence: Peter Fiener (peter.fiener@geo.uni-augsburg.de)

Abstract. In the last decades, soils and their agricultural management have received great scientific and political attention due to their associated potential to act as a sink of atmospheric carbon dioxide (CO_2). It is questioned if soil redistribution processes affect this potential CO_2 sink function, as agricultural management has a strong potential to accelerate soil redistribution. Most studies analysing the effect of soil redistribution upon soil organic carbon (SOC) dynamics focus on water erosion, analyse
5 only relatively small catchments and relatively short timespans of several years to decades. The aim of this study is to widen the perspective by including tillage erosion as another important driver of soil redistribution and performing a model-based analysis in a $200\,km^2$-sized arable region of north-eastern Germany for the period since the conversion from forest to arable land (approx. 1000 years ago). Therefore, a modified version of the spatially explicit soil redistribution and carbon (C) turnover model SPEROS-C was applied to simulate lateral soil and SOC redistribution and SOC turnover (spatial resolution 5 m x 5 m).
10 The model parameterisation uncertainty was estimated by simulating different realisations of the development of agricultural management over the past millennium. The results indicate that in young moraine areas, which are relatively dry but intensively used for agriculture for centuries, SOC patterns and dynamics are substantially affected by tillage-induced soil redistribution processes. To understand the landscape scale effect of these redistribution processes on SOC dynamics it is essential to account for long-term changes following land conversion, as typical soil-erosion induced processes, e.g. dynamic replacement, only
15 take place after former forest soils reach a new equilibrium following conversion. Overall, it was estimated that after 1000 years of arable land use, SOC redistribution by tillage and water erosion results in a landscape-scale C sink of up to 0.66‰ per year.

1 Introduction

Soils play an important role in the global carbon (C) cycle (Bellamy et al., 2005; Berhe et al., 2008; Lal, 2004) and have
20 received great scientific (e.g. Amelung et al., 2020; Bellassen et al., 2022; Van Oost et al., 2007) and political attention as one of the cornerstones to tackle climate change, e.g. 4‰ initiative (Minasny et al., 2017), Article 3.4 of the Kyoto Protocol (United Nations Framework Convention on Climate Change, 1998), and special report of the IPCC (Intergovernmental Panel on Climate Change, 2019).

A substantial loss of soil organic carbon (SOC) to the atmosphere before industrialisation is generally associated to the
conversion of (natural) forest sites to cropland (Lal, 2019; Le Quéré et al., 2016; Sanderman et al., 2017). However, tillage
operations and water erosion lead to an accelerated lateral redistribution of SOC within agricultural landscapes (Montgomery,
2007). In consequence, the spatial variability of SOC within soils of arable landscapes increase, but this also creates complex
interactions between changing SOC profiles, site-specific C mineralisation and sequestration, and potential losses to aquatic
ecosystems (Doetterl et al., 2016). In a nutshell, (i) the removal of SOC-rich topsoil at erosional areas stimulates dynamic
replacement of C via fresh photosynthates and the uplift of more reactive subsoil minerals (Harden et al., 1999; Stallard, 1998).
(ii) During transport by different erosion agents, some SOC might be mineralised due to erosion-induced aggregate breakdown
(Doetterl et al., 2016); however, this has a relatively short-lived effect, due to the episodic nature of erosion processes (Van Oost
and Six, 2023). (iii) At depositional sites, SOC is buried in deeper soil layers and hence is protected from fast mineralisation
(Berhe et al., 2008; Rumpel and Kögel-Knabner, 2011; Stallard, 1998). (iv) In case of water erosion, SOC will also partly enter
aquatic ecosystems, where it is either buried in sedimentary deposits or mineralised during fluvial transport (Aufdenkampe
et al., 2011; Battin et al., 2009).

The impact of soil redistribution on C dynamics has been assessed in various studies as reviewed in e.g. Doetterl et al. (2016),
Kirkels et al. (2014), and Van Oost and Six (2023). Such studies have often benefited from a strong modelling component, which
has been explored by both process-oriented models and more conceptual approaches. Most process-oriented studies focused
on water-erosion prone micro-catchments where field surveys regarding spatial patterns of SOC and erosion, or general erosion
monitoring, can be used for model development and testing (e.g. Doetterl et al., 2012; Van Oost et al., 2005; Wilken et al.,
2017a). The focus on small erosion-prone catchments has several implications: (i) results can only be partially generalised, as
these small-scale water erosion studies tend to be located in steeper areas; (ii) water erosion studies are often associated with
loess-burden soils (e.g. Dlugoß et al., 2012; Li et al., 2007; Wilken et al., 2017a), which, although highly erodible, are also
deep and display a low sensitivity to soil truncation regarding crop productivity; and (iii) the focus on water erosion makes it
difficult to close the C balance, as the fate of SOC after leaving the micro-catchment is open to debate (Aufdenkampe et al.,
2011; Battin et al., 2009; Van Oost and Six, 2023). Apart from these process-oriented studies, there are also regional (Lugato
et al., 2018; Nadeu et al., 2015) and even global (Naipal et al., 2018; Van Oost et al., 2007) model-based estimates of the effect
of soil redistribution on SOC stocks, which are based on coupled conceptual soil erosion and C turnover models. These (water
erosion) modelling studies give valuable insights for large areas but are mostly focused on current erosion and C turnover
(e.g. Nadeu et al., 2015; Van Oost et al., 2007), while long-term effects of erosion-induced C dynamics after centuries or even
millennia of land management are ignored. In consequence, model results might overestimate the effect of intensive modern
agriculture, as they typically only take the last 50 to 100 years into account (e.g. Dlugoß et al., 2012; Nadeu et al., 2015; Wilken
et al., 2017b). Only a few of these regional studies addressed longer time scales (e.g. Bouchoms et al., 2017; Wang et al., 2017),
which is a prerequisite to compare today's SOC soil profiles with model outputs in regions with a long agricultural land use
history.

However, such long-term regional erosion and C turnover modelling is obviously challenged through the rapid decline in
data accessibility and quality when moving back for centuries or even millennia. Apart from natural factors (e.g. climate,

topography, soil cover, soil development, etc.) it is most challenging to reconstruct factors governed by agricultural practices
60 (e.g. crop rotations, productivity, modification of soil cover, tillage methods, etc.). Moreover, estimates of initial (undisturbed) soil conditions (especially SOC stock profiles) are required to initiate long-term modelling. The existing long-term modelling studies (Bouchoms et al., 2017; Wang et al., 2017) used undisturbed soil profiles from long-term arable land, while to our knowledge studies accounting for the decline of SOC following conversion from forest to arable land in combination with erosion-induced C fluxes have not been carried out. Moreover, tillage erosion has been shown to be the main soil redistribution
65 process in different parts of the world (e.g. Gerontidis et al., 2001; Lobb et al., 1995; Van Oost et al., 2003) and ignoring its effects on long-term C dynamics might lead to spurious conclusions.

Any large-scale and long-term study faces the challenge of assumption-based input data. Hence, the aim of large-scale and long-term modelling must be to simulate plausible patterns instead of process-based reconstruction. The aims of this study are (i) to simulate long-term changes (1000 years) in soil profiles in an agricultural landscape heavily affected by tillage erosion
70 and less affected by water erosion; (ii) to perform a model-based soil redistribution and SOC turnover analysis for a larger area (about $200\,\text{km}^2$), in order to avoid a systematic bias typically found in small-scale studies focussing on erosion processes in steep areas; and (iii) to model the long-term effect of soil redistribution when moving from a SOC-rich forest soil to a heavily eroded arable soil after 1000 years of cultivation.

2 Materials and methods

75 ### 2.1 Study area

The study area covers an area of $196\,\text{km}^2$ and is located in the Quillow river catchment about $100\,\text{km}$ north of Berlin in north-eastern Germany (Figure 1). It represents a typical ground moraine landscape formed after the retreat of the Weichselian glaciers ca. 15,000 years ago (shaded area in Figure 1; Lüthgens et al., 2011). The area is characterized by a hilly topography with short summit-footslope distances (on average 35 m) and a mean slope ($\pm$ standard deviation) of ca. 4.4 % $\pm$ 3.7 %. A large
80 number of kettle holes that were formed by the delayed melting of bigger ice blocks (Anderson, 1998) are typical landscape elements. Drainage is only possible via sub-surface flow from the kettle holes (Lischeid et al., 2017). The kettle holes can be filled with water, (degraded) peat or are covered by colluvial material resulting from arable land use over centuries (Van der Meij et al., 2019).

The land cover of the study area is dominated by arable land and pasture (ca. 70 %), followed by wetlands and lakes (ca.
85 16 %), while only a small part is made up by forest (ca. 11 %) and settlements (ca. 3 %; Heinrich et al., 2018). Some parts of the study area have been used for agriculture since Neolithic times (ca. 5500 BCE; Behre, 2008), while it is assumed that agricultural land use became widespread approximately in 1000 CE (Behre, 2008; Herrmann, 1985). Intensive mechanisation of agriculture started in the second half of the 20th century. This was accompanied by a substantial increase of field sizes during the socialistic era of the German Democratic Republic (Bayerl, 2006), resulting in recent average field sizes of 21 ha ($\pm$ 20 ha).
90 The region is characterized by a relatively dry subcontinental climate with an average annual air temperature of 9.4 °C and
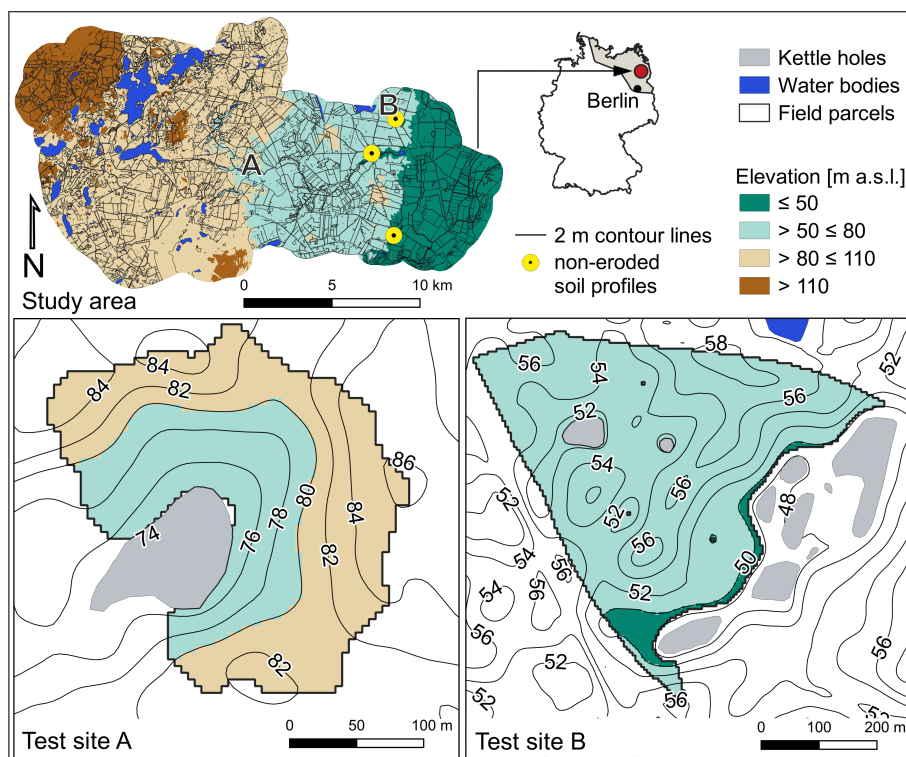
Figure 1. The study area is located north of Berlin in the young moraine landscape of north-eastern Germany indicated by the grey area of the inset map (upper panel). Location of the two test sites A and B (black letters) as well as of the four non-eroded soil profiles used for calibration (yellow circles) within the study area. Thereby, the yellow circle close to test site B represents two profiles. Topography and kettle holes of test site A (lower left panel) and B (lower right panel) with 2 m contour lines (black lines). The elevation of the test sites is shown by using the colour scheme of the upper panel.

a mean annual precipitation of 466 mm (20-year average 2001-2020, DWD meteorological station at Grünow; DWD Climate Data Center (CDC), 2018, 2021).

The soil pattern of the region follows the heterogeneity of Pleistocene deposits and has been strongly modified by soil redistribution over the past centuries (Deumlich et al., 2010; Sommer et al., 2008; Koszinski et al., 2013). Nowadays, non-eroded soils can only be found at ca. 20 % of the arable land, mainly at lower midslopes or flat plateaus. Thereby, extremely eroded soils occur at hilltops, ridges, and slope shoulders, while strongly eroded soils are found from slope shoulders to upper midslopes. Groundwater-influenced colluvial soils have developed at footslopes of closed depressions, which are often covering fossil peat (see more details in Öttl et al., 2021).

Within the Quillow study area two agricultural fields (Figure 1) were chosen to test the plausibility of the modelling results (i.e. current estimates of SOC stocks and patterns). They were selected because of existing SOC data from previous studies (e.g. Wehrhan and Sommer, 2021; Wilken et al., 2020). Test site A is located approximately in the centre of the study area

(53.3550° N, 13.6643° E), has a size of ca. 4.4 ha and a mean slope of 8.7 % ± 3.9 %. Test site B is in the northeast of the study area (53.3836° N, 13.7818° E), has an area of ca. 20.5 ha and a mean slope of 5.5 % ± 2.9 %.

2.2 Modelling approach

105 A modified version of the spatially explicit soil redistribution and C turnover model SPEROS-C (Dlugoß et al., 2012; Fiener et al., 2015; Van Oost et al., 2005) was applied for modelling tillage- (TIL) and water-induced (WAT) soil redistribution in the mesoscale study catchment over the past millennium. Thereby, lateral soil and SOC redistribution, SOC turnover, and vertical mixing within the profile (spatial and vertical resolution 5 m x 5 m and 10 x 0.1 m soil depth increments, respectively) were simulated. To isolate C fluxes that occur solely due to total soil redistribution (TOT is the sum of TIL and WAT), a reference

110 run simulating C fluxes without soil redistribution was calculated. Modelling soil redistribution and C dynamics required estimating and calibrating model input parameters and their uncertainty, as well as evaluating the model outputs. The single steps are described in detail in the following section.

2.2.1 Modelling soil redistribution and SOC dynamics

Tillage-induced soil redistribution. TIL is calculated based on a diffusion-type equation developed by Govers et al. (1994)

115 (Eq. 1). The net soil flux due to tillage Q_{til} (kg m^{-1} yr^{-1}) can be written as

$$Q_{til} = -k_{til} \cdot s = -ktil \cdot \frac{\delta h}{\delta x}, \tag{1}$$

whereby k_{til} is the tillage transport coefficient (kg m^{-1} yr^{-1}), s is the local slope (%), h is the height at a given point of the hillslope (m), and x is the soil translocation distance in horizontal direction (m). The local tillage-induced soil redistribution rate E_{til} (kg m^{-1} yr^{-1}) is calculated as

120 $$E_{til} = -\frac{\delta Q_{til}}{\delta x} = -ktil \cdot \frac{\delta^2 h}{\delta x^2}. \tag{2}$$

Thereby, the intensity of the calculated erosion rates is determined by the k_{til} and the change in slope gradient determines the spatial pattern of tillage-induced soil redistribution.

Water-induced soil redistribution. WAT is calculated according to a slightly modified approach of the Revised Universal

125 Soil Loss Equation (RUSLE; Renard et al., 1997), which is described in detail in Van Oost et al. (2000). A local transport capacity T_c (kg m^{-1} yr^{-1}; Eq. 3) determines whether erosion, sediment transport, or deposition occurs. If the sediment inflow is higher than T_c the excess is deposited, while the T_c is further routed downstream.

$$T_c = k_{tc} \cdot P \cdot C \cdot K \cdot R \cdot LS_{2D}, \tag{3}$$

whereby k_{tc} is the transport capacity coefficient (m), P, C, K, and R are the RUSLE factors, and LS_{2D} is a grid-cell specific
130   topographic factor calculated following Desmet and Govers (1996).

SOC turnover model. SOC stocks are modelled for a soil profile with 10 soil layers of 0.1 m. The model equations describ-
ing the SOC depth profile and SOC decay are based on the Introductory Carbon Balance Model (ICBM; Andrén and Kätterer,
1997; Kätterer and Andrén, 1999). ICBM considers a young (Y) and old (O) C pool with different turnover rates ($k_Y = 0.8\,\text{yr}^{-1}$,
135   $k_O = 0.006\,\text{yr}^{-1}$). The fraction of the annual flux from Y to O is determined by the humification coefficient h. External environ-
mental factors from climate and soils are combined in the factor r and the mean annual C input to the soil is represented by
the parameter i (Andrén and Kätterer, 1997). The dynamics of the two SOC pools are described by the following differential
equations (Andrén and Kätterer, 1997):

$$\frac{\delta Y}{\delta t} = i - k_y \cdot r \cdot Y, \tag{4}$$

$$\frac{\delta O}{\delta t} = h \cdot k_y \cdot r \cdot Y - k_O \cdot r \cdot O, \tag{5}$$

SOC turnover rates are assumed to decrease exponentially with depth due to a decreasing influence of environmental condi-
tions (Eq. 6; Rosenbloom et al., 2001).

$$k_{Y/Oz} = k_{Y/Oz} \cdot e^{(-u \cdot z)} \tag{6}$$

Annual C input i ($\text{g C m}^{-2}\,\text{yr}^{-1}$) is derived from crops (i_c) and manure (i_m; Eq. 7). Thereby, i_c is made up by an above- and
145   a belowground component. Crop residues are determined by the residue to aboveground biomass (*AGBM*) ratio (*Res*). The
fraction of C input from roots and rhizodeposition (p_z) at a given soil depth z (m) is defined by the root to *AGBM* ratio (*RS*).
For i_c, a C content (C_{cont}) of 0.45 is used (Eq. 8; Tum and Günther, 2011).

$$i = i_c + i_m \tag{7}$$

$$i_c = C_{cont} \cdot [(Res \cdot AGBM) + (p_z \cdot RS \cdot AGBM)] \tag{8}$$

150   The C input into the soil is modelled by assuming an exponential root density profile (Gerwitz and Page, 1974; Van Oost
et al., 2005), while manure input is only assigned to the plough layer (or layers). The allocation of total root dry matter to each
soil layer z (m) was calculated according to a reference soil depth $z_r = 0.25\,\text{m}$ (Van Oost et al., 2005) and a constant c that
determines the proportion of the roots per soil layer (p_z; Eq. 9).

$$for\ z \le z_r : p_z = \frac{z}{z_r + \frac{1 - e^{-c(1 - z_r)}}{c}}$$

155 $$for\ z > z_r : p_z = \frac{z_r + (1 - e^{-c(z - z_r)})/c}{z_r + (1 - e^{-c(1 - z_r)})/c} \tag{9}$$

The humification coefficient h is weighted according to the proportion of the source of i and depends on clay content cp (%) (Eq. 10; Kätterer and Andrén, 1999).

$$h = \frac{i_c \cdot h_c + i_m \cdot h_m}{i} \cdot e^{0.0112 \cdot (cp - 36.5)} \tag{10}$$

The temperature response factor r that accounts for the environmental influence on SOC decay is calculated with the follow-
160 ing exponential Q_{10} function (Kätterer et al., 1998; Van Oost et al., 2005):

$$r = Q_{10} \frac{T - 5.4}{10}. \tag{11}$$

Thereby, r is estimated with a Q_{10} value of 2.07 (Kätterer et al., 1998), a temperature T (°C) calibrated for this study (as described below), and by correcting temperature by the annual mean temperature of central Sweden (+ 5.4 °C) (Andrén and Kätterer, 1997).

165

Soil profile update. After every time step the SOC profile is updated considering yearly soil loss and gain due to water and tillage erosion. At eroding sites, a fraction of SOC from the first subsoil layer equal to the thickness of the eroded layer is incorporated into the plough layer. At depositional sites, a fraction of the SOC from the plough layer is shifted downwards into a buried plough layer. The underlying subsoil layers are further buried according to the depth of the soil deposition in that time
170 step (Dlugoß et al., 2012; Van Oost et al., 2005).

To account for the development of tillage implements and practices (Figure 2 a, Table A1), plough depth was updated with time, but kept constant through periods without significant changes in historical plough development. Based on a literature review, we changed plough depth from 0.1 m for the first 800 years of the model simulations to 0.2 m for 1800-1900 CE and to 0.3 m for 1900-2000 CE (Figure 2 c). The yearly vertical C fluxes are then calculated following the profile update.

175 ### 2.2.2 Model implementation

One of the major challenges in performing a model-based analysis of the impacts of 1000 years of soil erosion upon C fluxes in an area of 200 km^2 is to estimate reasonable model inputs and to determine appropriate model parameters. Obviously, this is associated with large uncertainties and requires substantial simplifications. It is important to note that the model allows a reasonable analysis of the importance of soil redistribution for the C balance of the entire study area, but it is not expected to
180 exactly mimic the current observational data.

Model realisations. Due to the uncertainties in the main model input parameters for the erosion modelling and to account for a varying importance of TIL and WAT, we created nine model realisations (R1 - R9). The realisations were simulated by a combination of a low, medium, and high water erosion pathway indicated by the minimum, the mean and the maximum values of the *C*, *K*, and *R* factors as shown in Figure 2 b, with a low, medium, and high tillage erosion pathway using the different
185   k_{til} values from Figure 2 a. The theoretical background that led to the erosion pathways is explained in detail in the next paragraphs. It is important to note that the variation in TIL and WAT is set to the relative importance of tillage and water erosion in the region as determined in earlier studies (Öttl et al., 2021; Wilken et al., 2020). The nine realisations are: (R1) low TIL, low WAT; (R2) low TIL, medium WAT; (R3) low TIL, high WAT; (R4) medium TIL, low WAT; (R5) medium TIL, medium WAT; (R6) medium TIL, high WAT; (R7) high TIL, low WAT; (R8) high TIL, medium WAT; and (R9) high TIL, high WAT.
190   Due to the large computing requirements in simulating 1000 years for roughly 8 x 10^6 raster cells of the entire study area, we only modelled the different realisations for the test fields (Figure 1, together roughly 10 x 10^3 raster cells). The most plausible realisation (as defined below) was later on used to model the entire study area.

Tillage-induced soil redistribution. A comprehensive literature review (comprising 47 original publications representing
195   137 k_{til} values; Table A1) was performed to assess tillage erosion intensity of different soil cultivation techniques. According to the land use history of the study region, the model period was subdivided into five periods representing different soil cultivation techniques.

For the first period (1000-1100 CE), the median k_{til} of 98 kg m^{-1} (min. 9 kg m^{-1}, max. 300 kg m^{-1}) was calculated from 23 k_{til} values for manual hoeing or the use of a simple ard (Table A1). Although the medieval mouldboard plough was already
200   invented around 200-900 CE (Van der Meij et al., 2019), it was assumed that the majority of the farmers still practiced manual hoeing or used the simple ard plough in the first period (Behre, 2008; Herrmann, 1985).

For the second period (1100-1800 CE) it was assumed that an increasing number of farmers used a rudimentary chisel or mouldboard plough drawn by an animal, as the turning plough was introduced around 1000 CE (Behre, 2008; Herrmann, 1985). As not much further information is available until the end of the 18th century, we used a set of 30 k_{til} literature values
205   representing ard, chisel or mouldboard plough drawn by a single animal. The median k_{til} of these studies is 88 kg m^{-1} (min. 14 kg m^{-1}, max. 300 kg m^{-1}; Table A1).

The fourth period (1800-1900 CE) was characterised by the industrial revolution that tremendously changed the way land was managed. From 1800 onwards the so-called "Ruchadlo", a steep turning tipping plough (Herrmann, 1985), and the "Mecklenburgischer Haken" for seedbed preparation were used (Behre, 2008). Both implements were pulled by animals (oxen or
210   horses). A median k_{til} of 100 kg m^{-1} (min. 14 kg m^{-1}, max. 300 kg m^{-1} was calculated from 15 k_{til} values for an ard, chisel or mouldboard plough pulled by one or two animals (Table A1).

The last period (1900-2000 CE) is characterized by the introduction of automotive tractors that were able to pull heavy implements and in consequence the ploughing depths increased to 20 - 40 cm (Behre, 2008; Bork et al., 1998; Van der Meij et al., 2019). The median k_{til} of 234 kg m^{-1} (min. 13 kg m^{-1}, max. 900 kg m^{-1}) was calculated from 69 k_{til} values for tractor-pulled
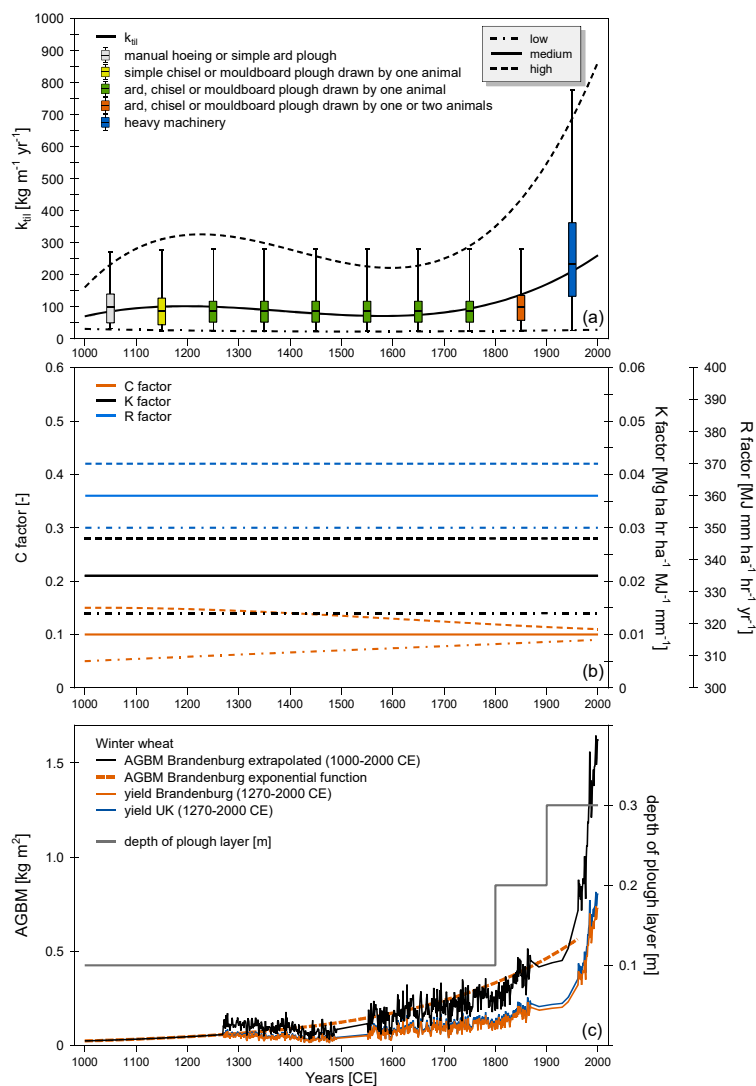
Figure 2. Range of reasonable input parameters for modelling tillage- (a) and water-induced soil redistribution (b), and SOC dynamics (c) for the model period of 1000 years. The range of parameters in (a) and (b) (dashed-dotted for the lower and dashed lines for the upper range, respectively; solid line represents the mean) is used in the different model realisations. Please notice the different scales of the y-axes. Abbreviations: k_{til} = tillage transport coefficient, *AGBM* = aboveground biomass; *C*, *R*, and *K* factor= factors of the RUSLE (Eq. 3). Information on data sources and explanation of the parameters can be found in the text.

215   heavy machinery (early and recent chisel and mouldboard plough, harrow, cultivator, tandem disc, etc.; Table A1).

Water-induced soil redistribution. A range of *C* factor values was estimated to represent the changes in crop cover/management throughout the simulation period (Figure 2 b). As such, two different conditions were assumed: for the upper limit of the parameter space it is assumed that the crop cover was low (i.e. high *C* factor) at the beginning of the simulation period
220 due to relatively lower yields and high row spacing. For the lower limit it is assumed that a much lower historic *C* factor might be reasonable due to a high vegetation cover related to a high proportion of weeds and grasses between the crops, which decreased over time due to improved weeding methods. To account for this uncertainty over time, we assumed that at 1000 CE the *C* factor might be either 50 % higher or lower than the current mean value. This range decreased according to a polynomial function (degree = 3) until reaching ± 10 % of the current value in 2000 CE. The current mean *C* factor of 0.1 was calculated
225 assuming a small-grain crop rotation (e.g. winter wheat – winter wheat – winter barley – winter rapeseed) typically applied under today's conditions (Deumlich et al., 2002; Öttl et al., 2021; Schwertmann et al., 1987).

The soil erodibility factor *K* was assumed to remain constant throughout the simulation period and was calculated based on a soil group map (Bundesministerium der Finanzen, 2007; Rust, 2006), following the approach as described in DIN ISO (19708:2017-08). The area-weighted mean *K* factor of 0.021 Mg ha hr ha⁻¹ MJ⁻¹ mm⁻¹ was used as medium realisation (Fig-
230 ure 2 b). The lower and upper parameter values used for creating the model realisations are the area-weighted mean plus-minus the standard deviation of the *K* factor, respectively (0.021 ± 0.007 Mg ha hr ha⁻¹ MJ⁻¹ mm⁻¹).

The rainfall erosivity factor *R* was calculated based on a long-term precipitation reconstruction for Europe (1500-2000 CE; Pauling et al., 2005) and an approach of Diodato et al. (2017) developed to estimate long-term erosion changes from historic precipitation data. As no precipitation data was available for the period 1000-1500 CE, the mean *R* factor of the available
235 data (362 MJ mm ha⁻¹ hr⁻¹ yr⁻¹ for 1500-2000 CE) was used as mean for the whole modelling period (Figure 2 b). To address a potential range in the *R* factor we used the mean ± 95 % confidence interval (362 ± 8.3 MJ mm ha⁻¹ hr⁻¹ yr⁻¹; Figure 2 b).

For this study, a constant transport capacity coefficient k_{tc} of 150 m was used as this value was found to be suitable for cropland and a grid resolution of 5 m x 5 m (Dlugoß et al., 2012; Van Oost et al., 2003). The grid cell-specific topographic factor LS_{2D} was calculated based on a digital elevation model (DEM; derived from airborne laser scanning; original spatial resolution
240 of 1 m resampled to 5 m; Landesamt für Umwelt, Gesundheit und Verbraucherschutz Brandenburg & Landesvermessung und Geobasisinformation Brandenburg, 2012). The support practice factor *P* is 1.0 for all realisations for the whole modelling period as no erosion control practices are assumed.

Both water and tillage erosion are sensitive to field sizes and layouts, which according to historic maps and later aerial photographs substantially changed over time. As we could not reconstruct field layout over one millennium for the entire test
245 area, it was decided to use recent field layouts. However, as the recent fields are very large this leads to an underestimation of potential field border effects.

SOC turnover and C balancing. To model SOC dynamics over 1000 years, SPEROS-C needs yearly estimates of C inputs based on *AGBM* as well as estimates of ploughing depths (Figure 2 c), as these variables change the C incorporation into the
250 soil. To calculate the temporal evolution of *AGBM* (Figure 2 c), yield data for the federal state of Brandenburg from 1950 until 2018 CE (Federal Statistical Office, 1990-2018; Staatliche Zentralverwaltung für Statistik, 1956-1990) was combined with a

Table 1. Model input parameters for modelling SOC dynamics in agricultural soils determined by Monte Carlo simulations (n = 1000). The initial values are varied by ± 10 % for sampling and the final value is the parameter set that yielded the highest Nash Sutcliffe model efficiency. The references proof that the initial values and their ranges are valid assumptions.

Calibrated parameter	Abbreviations used in the text	Unit	Initial value	Final value	Reference for initial value
Clay percentage	cp	%	13.0	14.0	Sommer et al. (2020)
Constant that defines root growth	c	–	4.0	3.62	Van Oost et al. (2005)
Decomposition depth attenuation	u	–	3.0	2.99	Van Oost et al. (2005)
Manure input	m	kg m^{-2}	0.05	0.05	Verch (2020)
Root:shoot ratio	RS	–	0.16	0.16	Herbrich et al. (2018)
Reference soil depth	z_r	m	0.25		Van Oost et al. (2005)
Residue to *AGBM* ratio	Res	–	0.1	0.11	Dlugoß et al. (2012)
Temperature	T	°C	8.0	7.9	DWD Climate Data Center (CDC) (2018)
Depth of plough horizon	–	m	0.3		Behre (2008); Herrmann (1985)

long-term winter wheat yield dataset of the UK (1270-2014 CE; Ritchie and Roser, 2013). Yield was converted to *AGBM* by multiplying with the harvest index (*HI*; Donald and Hamblin, 1976), which determines the proportion of yield to total biomass for specific crop species. The *HI* was calculated with winter wheat grain and straw data from Brandenburg (mean *HI* = 0.449;

255 Kuratorium für Technik und Bauwesen in der Landwirtschaft e. V. (KTBL), 1951, 1970, 1980, 1993, 2005). We assumed that for every third year of the simulation the *AGBM* would not be harvested, in order to account for the so-called "three-field economy" (Rösener, 1985; Volkert, 1991), i.e. a crop rotation regime commonly used in Germany since medieval times and in which a field was left fallow every third year.

While changes in *AGBM* and ploughing depths can be reasonably estimated based on existing data, it is hardly possible

260 to estimate the temporal (or even spatial) variability of other model parameters, e.g. root:shoot ratio, manure application etc., used in ICBM. Therefore, we used SOC depth distributions from four standard soil profiles representing undisturbed (i.e. non-eroded) arable soils in the study area (soil database of ZALF e.V. and Sommer et al. (2020)) and values from the literature as initial model parameters (Table 1).

These were later optimised to derive a model parameter set used for the entire modelling period. That is, first we varied the

265 literature parameter values one-at-time until they matched the observation data (i.e. combination of the four non-eroded SOC depth profiles; orange line in Figure 3). Second, the obtained representative initial values for the observed SOC profile were used in a Monte Carlo simulation (n = 1000). Each parameter was sampled from a uniform distribution in a range of ± 10 % around its initial value, which resulted in 1000 different modelled SOC-depth profiles. Hence, not only the direct influence
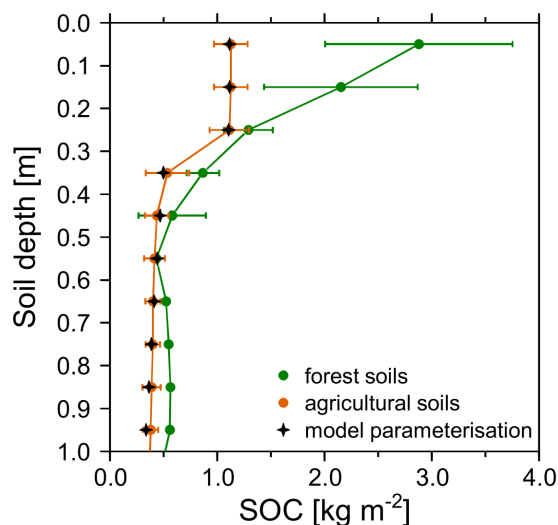
Figure 3. Depth profile of the mean observed SOC stocks for the forest (green) and agricultural soils (orange) with error bars of ± one standard deviation. The forest soils are used as initial soil condition, while the calibration of the agricultural soils is used as parameterisation for modelling the 1000 years (black stars).

of each parameter on the model output was considered but also the joint influence due to interactions between the parameters

270 (Pianosi et al., 2016). The parameter set which yielded the highest Nash-Sutcliffe model efficiency (Nash and Sutcliffe, 1970) was selected for the final modelling (black stars in Figure 3).

Model evaluation. A straightforward, traditional model-testing approach of the correspondence between observational data and model outputs after simulating 1000 years of soil redistribution and C turnover in a study area of about 200 km² is obviously

275 hardly possible. There are neither commensurate quantitative measurements of erosion available at this spatiotemporal scale, nor is it appropriate to directly compare soil truncation or SOC patterns of individual fields with a model output based on a parameterisation for the entire study area. As such, we focused on an investigative model evaluation approach (Baker, 2017), in which two independent datasets were used to evaluate the model's capability to consistently represent the long-term erosion-induced C balance for the study area.

280 The first independent data used for model evaluation was derived from a remote sensing approach for identifying spatial patterns of severe soil erosion and soil truncation. Typical features in the study area are signs of soil truncation at hilltops, which most likely result from prolonged tillage erosion (Deumlich et al., 2010; Sommer et al., 2008). The heavily eroded hilltops are visible in remote sensing data due to their brighter colours resulting from an exposure of the subsoil horizon partly consisting of glacial till (Figure 4).

Figure 4. Exemplary aerial photos of the study area showing eroded hilltops as indicated by the lighter soil colours. Notice that the aerial photo to the left was taken in 1953 (© ZALF e.V.), while the one to the right is from 06/09/2016 (© Google).

285   Heavily eroded areas can be straightforward detected by using remote sensing data for the entire catchment area. Therefore, 24 multispectral Sentinel-2 satellite images (ESA, 2015) acquired during bare soil conditions were classified (support vector machine tool; ArcGIS version 10.7.1). As the classification can only be performed for fields with bare soil conditions at the time of satellite image acquisition, about 21 % of the study area (ca. 1.7×10^6 raster cells) was classified, whereby 6 % of the study area were classified as heavily eroded (ca. 4.2×10^5 raster cells). As hilltop erosion might also lead to a movement of the

290 surface-exposed subsoil into the surrounding areas not affected by erosion, a buffer of -5 m was created to the inside of the area resulting in 5.2 km^2 or 2.1 x 105 raster cells classified as heavily eroded. These raster cells are used to evaluate the consistency of the modelled erosion patterns, which have been shown to be dominated by tillage erosion in a previous study (Wilken et al., 2020).

    The second source of independent model-evaluation data was derived from measured SOC stocks for two different test sites

295 in the study area. For test site A (Figure 1), plough layer SOC stocks are available from a nested sampling design (20 m x 20 m; see Wilken et al., 2020) carried out in 2018. The data were geostatistically interpolated using a kriging approach to a regular grid with 5 m x 5 m resolution. At test site B (Figure 1), the topsoil SOC stocks were derived from a regression analysis of ground truth SOC measurements (first 0.15 m) against multispectral images taken by a remotely piloted aircraft system (Wehrhan and Sommer, 2021). Both observed SOC patterns were compared to model outputs.

300 **3   Results**

3.1   Model evaluation

A comparison between modelled and remotely sensed soil redistribution patterns (Table 2) indicated that the most severely eroded sites were associated with tillage induced (TIL) and total soil redistribution (TOT). Overall, about 81 % of the areas classified as heavily eroded according to the remote sensing approach correspond to the modelled erosion class. On average

305 those areas show a modelled soil loss of -0.23 mm yr^{-1} (R4), most of which was caused by tillage erosion (Table 2).

Table 2. Agreement between modelled WAT, TIL and TOT erosion classes and remote sensing derived erosion classification. Note that a threshold of -0.05 mm erosion per year was used to exclude areas with minimal erosion after modelling 1000 years of soil redistribution. The area classified from the remote sensing data represents about 21 % of the entire study area. Within the classified area, about 28 % is heavily eroded (about 4.7×10^5 raster cells).

Erosion type	Agreement [%]	Mean erosion rate [m] ± one standard deviation
Total erosion (TOT)	81.21	-0.23 ± 0.14
TIllage erosion (TIL)	76.00	-0.22 ± 0.13
Water erosion (WAT)	11.63	-0.08 ± 0.03

A visual comparison of modelled erosion against observed topsoil SOC patterns of the two test fields (A and B; Figure 5) shows an obvious relation between the observed SOC patterns and tillage erosion. This finding is further supported by a comparison of modelled topsoil SOC stocks based on the nine model realisations, which underlines that the quality of the results is mostly determined by the differences in tillage erosion intensity (Figure 6). Best results in respect of the used goodness-of-

310 fit parameters can be reached for the medium (R4 - R6) and high tillage erosion realisations (R7 - 9), whereas the medium and high TIL realisation fits better for test site A and B, respectively (Figure 6). In contrast, WAT plays only a minor role in explaining the spatial distribution of SOC. It is important to note that especially in case of test site B, where topsoil SOC stocks are estimated with a remote sensing approach, the model substantially underestimates the SOC contents. Taking this into consideration, while also trying to perform a somewhat conservative estimate of the extent of tillage erosion, we used

315 realisation R4 (medium TIL, low WAT) for the following model analysis of the entire study area.

3.2 Results of modelling erosion-induced C-flux dynamics for 1000 years

The modelled C fluxes without soil redistribution indicated a C loss to the atmosphere following conversion to arable land for about the first 800 years of the simulation (Figure 7 a, b; *w/o soil redistribution*), with some interannual variability of vertical C fluxes due to the three-field economy (i.e. crops left on the field every third year). The resulting decrease in SOC stocks

320 (Figure 7 e) was more pronounced for the first 500 years, nearly reaching a new equilibrium around 1700 CE. Soils turned into a slight C sink in the beginning of the 19th century, after an abrupt change in modelled plough depth from 0.1 to 0.2 m. This changed again at the beginning of the 20th century after the modelled plough depth was increased to 0.3 m and especially after the end of the three-field economy, which substantially reduced the modelled soil C input (Figure 7 a, b; *w/o soil redistribution*). Finally, soils turned into a C sink again after 1950 due to the extremely increasing yields (associated with a substantial increase

325 in soil-C input) following the end of the Second World War (Figure 7 c).

Based on the model simulations with the representation of lateral soil redistribution processes, we found that at erosional sites (Figure 7 a) the C loss to the atmosphere was less pronounced compared to sites without soil redistribution, and from
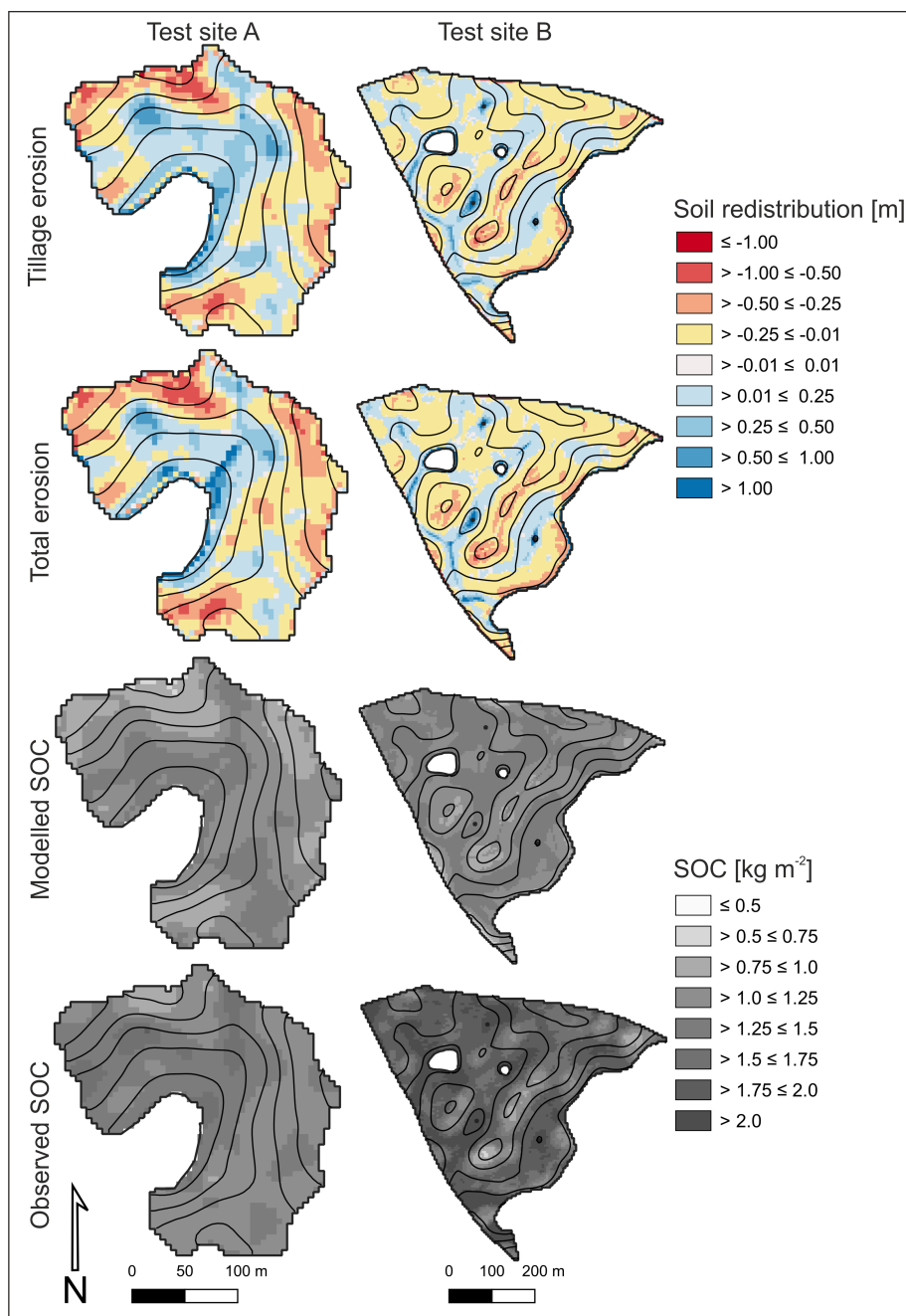
Figure 5. Modelled spatial patterns of tillage-induced (first row) and total soil redistribution (second row) at the end of the 1000 years simulation period. Modelled (third row) and observed topsoil (first 0.1 m) SOC (last row). For the two test sites A (left) and B (right). Model results are produced with realisation R4 (medium TIL and low WAT). Black lines indicate 2 m contour intervals.
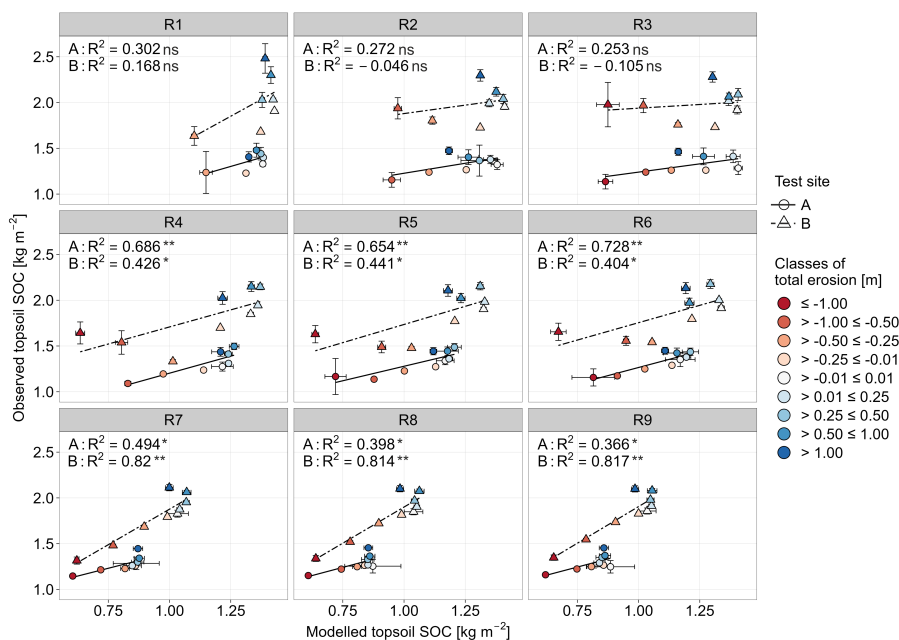
Figure 6. Modelled versus observed topsoil (first 0.1 m) SOC stocks for the two test sites A (circles) and B (triangles) and the nine realisations (in panels). Data is grouped into classes of total soil redistribution ranging from extreme erosion ($\leq$ -1 m, red) to high deposition ($\geq$ 1 m, blue). Error bars indicate the 95 % confidence interval of the mean per class. Black lines show the regression of the classified data (solid for A, dashed for B) with the respective adjusted coefficient of determination (R^2; ns = p-value $\geq$ 0.05, * = p-value < 0.05 and $\geq$ 0.01, ** = p-value < 0.01).

about 1550 CE onwards eroded soils became a C sink. From this time onwards the C sink function steadily increased until 1900 CE, when it dropped due to changes in soil C input (i.e. end of the three field economy). The C sink function at eroding positions increased more pronouncedly again in the 20th century compared to sites without soil redistribution until the end of the modelling period.

Moreover, the simulations considering lateral soil redistribution processes revealed a decrease in vertical C fluxes in depositional sites, compared to the simulations without soil redistribution (Figure 7 b). Such differences became more pronounced over time, as increasingly more C was stored in colluvial soils. It is important to note that deep C burial (> 1 m soil depths) did successively become more important for the vertical C fluxes over time (Figure 7 b), whereas the increase in C mineralisation in the upper 1 m of depositional sites (first order kinetics) was reduced by deep burial. This is especially important in case of prolonged severe deposition, as more and more C-rich former topsoil is moving to depths below 1 m.

The simulated lateral C export due to water erosion (Figure 7 d; exp_{tot}) in the test region was very small, especially since a new SOC equilibrium under arable land is reached. For approximately the first 200 years of the simulation, the C export steadily decreased as the SOC content of the topsoil being eroded substantially declined following land-use conversion. For about the next 600 years the modelled export steadily increased due to rising water erosion rates, as we assumed an increase
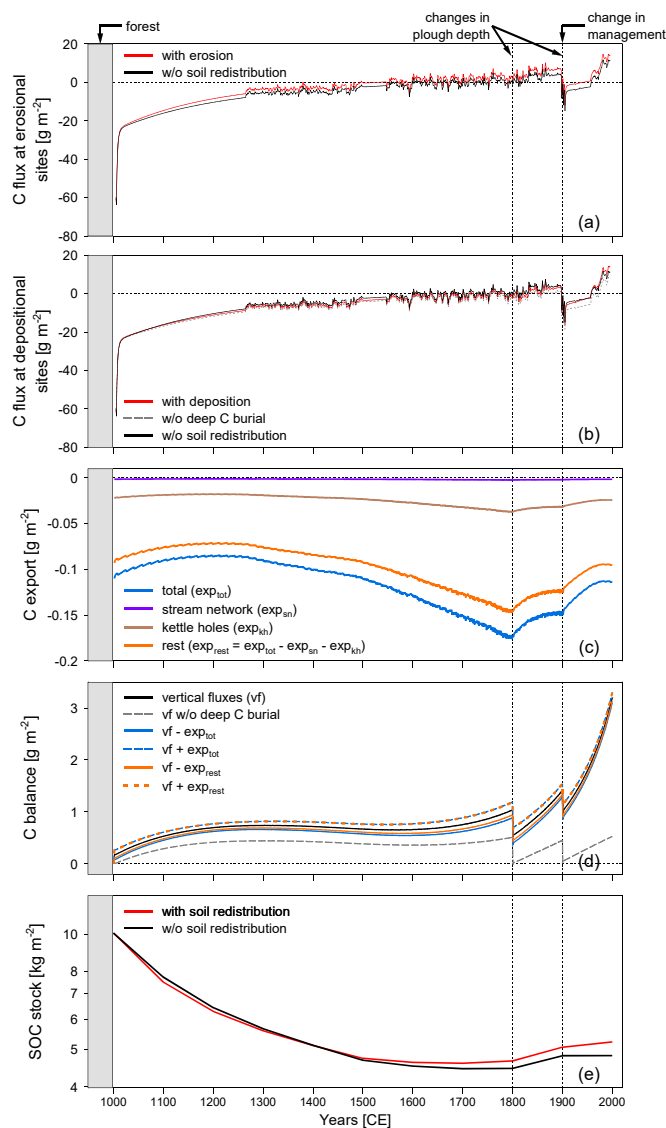
Figure 7. Temporal variation (1000 years) of annual vertical C fluxes, lateral C export, C balance, and SOC stocks modelled for the study region (R4) following conversion from forest to agricultural land (grey boxes). Plough depth was increased from 0.1 to 0.2 m and to 0.3 m in year 1800 and 1900, respectively (vertical dotted lines). Until 1900, *AGBM* was left on the field every third year. Vertical C fluxes at erosional (a) and depositional sites (b), total lateral C export (c), soil redistribution-induced C balance of all modelled fluxes (d), and mean soil SOC stocks of the entire study area (e; log-scaled y-axis). Notice that negative vertical C fluxes indicate a loss of C to the atmosphere, while positive C fluxes indicate a gain in soil C.

in the C factor for the period in the low water erosion pathway (Figure 7 b; R4) used to analyse the entire study area. At the beginning of the 19th and 20th century, respectively, the increase in ploughing depth led to a reduction of the topsoil SOC content and hence less C export via water erosion.

345   Based on the conservative assumption that all lateral C fluxes leaving arable land were lost to the atmosphere (Figure 7 d; $vf-exp_{tot}$), soil redistribution resulted in a steadily increasing C sink of about $3\,\mathrm{g\,C\,m^{-2}\,yr^{-1}}$ at the end of the modelling period. This sink function is only slightly more pronounced if we assume that most C exported from arable land into neighbouring land uses or into kettle holes was stored and not mineralised, while only the proportion entering the stream network was lost to the atmosphere (Figure 7 d; $vf-exp_{rest}$). Especially in the last two centuries of the simulation, deep C burial became more

350   important for the entire soil redistribution-induced C balance of the study area (Figure 7 d; *vf w/o deep C burial*).

The sum of all C fluxes with and without lateral soil redistribution is also mirrored in the changes of the mean SOC stocks of the study area (Figure 7 e). Here it is interesting to note that for about the first 300 years after conversion to arable land, soil redistribution led to a faster decline in SOC stocks compared to the system without soil redistribution. After about 500 years the reverse was simulated, leading to a mean difference between mean SOC stocks with and without redistribution of about

355     $0.42\,\mathrm{kg\,C\,m^{-2}}$ (8.7 %).

4   Discussion

4.1   Challenge of long-term soil redistribution and C turnover modelling

Understanding current agricultural soil-landscape relations requires to consider the long-term soil change, as today's soil and SOC patterns cannot be explained via the short-term soil redistribution history. The importance of long-term soil redistribu-

360   tion processes in agricultural landscapes is particularly obvious in the Quillow catchment, as our results have demonstrated. Although soil redistribution in the study area increased with the intensive agricultural mechanisation since the 1960s (Frielinghaus and Vahrson, 1998), this does not explain the observed erosion rates and patterns in the area (Wilken et al., 2020), especially at slope shoulders, where signs of tillage erosion are clearly visible in aerial photographs from the 1950s (Figure 4, left). A comparison between our results with typical soil truncation and accumulation rates for the study area (Van der Meij

365   et al., 2017) shows that it is necessary to consider the past millennium (i.e. since the beginning of agricultural management) to understand the landscape C dynamics.

However, any long-term and particularly landscape-scale modelling approaches are subject to considerable uncertainties. Here we did not intend to mimic detailed observational data of lateral soil fluxes (which are in any case not available at a commensurate temporal resolution to our model outputs) from individual sites of the $200\,\mathrm{km^2}$ study area with a high degree

370   of accuracy and precision. On the contrary, our investigative model evaluation approach was focused on testing the model's consistency for simulating long-term, landscape-scale spatial patterns of soil truncation and SOC stocks, while partially representing the uncertainties associated with parameter estimation in such an ambitious modelling experiment. As such, a set of model realisations (Figure 2; Figure 6) that combined different soil-redistribution assumptions were considered. The entire study area was ultimately analysed following the model realisation R4 (i.e. medium tillage and low water erosion), which

375 could explain 69 % and 43 % (see R^2 in Figure 6) of the current spatial pattern of SOC stocks in test sites A and B (Figure 1; Figure 5). This leads to an underestimation of the mean SOC stocks by 40 % and 20 % in the topsoil of test site A (50 cm soil depth) and B (plough layer), respectively. Importantly, the model outputs displayed a high agreement (81 %) with independent data used for estimating areas of severe soil truncation.

Overall, these results are encouraging, considering that (i) we only calibrated C-turnover parameters, while the tillage and
380 water erosion components of the model were applied 'blindly' to derive a set of plausible realisations for the whole study area; (ii) the model was parameterised to represent the average conditions in the entire study area, not accounting for the anyway unknown specific land use and management history of the individual test sites; and that (iii) in the relatively rare cases in which soil erosion models have been tested against independent spatial data, results have generally shown a poor agreement with observational data (Batista et al., 2019). As such, our modelling outputs are consistent with independent lines of evidence of
385 related phenomena and with our current understanding of long-term soil- and SOC-redistribution processes at landscape scale. This corroborates the usefulness of the employed modelling approach for elucidating soil redistribution and C dynamics in the study area over the last 1000 years.

4.2 Long-term soil redistribution and C dynamics

This model-based analysis of the long-term, landscape-scale effects of soil redistribution following land conversion from forest
390 to arable land upon C dynamics extends previous studies that mostly combine soil redistribution with SOC turnover over shorter time periods, smaller areas, and were based on soils that are already in C equilibrium due to long-term arable use (e.g. Dlugoß et al., 2012; Nadeu et al., 2015; Wilken et al., 2017b). Taking the conversion from forest to arable land into account clearly indicates that time since conversion is essential for the understanding of soil redistribution-induced C fluxes, which was to the best of our knowledge not included in previous long-term modelling studies (e.g. Bouchoms et al., 2017; Wang
395 et al., 2017). Our results demonstrate that there is no dynamic replacement at erosional sites as long as topsoil soils still lose C following conversion from SOC-rich forest to SOC-depleted arable soils. This is particularly important as dynamic replacement is assumed to be one of the key processes for a potential C sink function of soil erosion (Doetterl et al., 2016; Harden et al., 1999). Within our simulation it took about 500 years until eroded soils in the study region started to act as C sink (Figure 7 a). This period would be substantially shorter in smaller, more erosion-prone catchments where SOC-rich topsoil from former
400 forested areas is lost faster (Dlugoß et al., 2012; Juřicová et al., submitted; Wilken et al., 2017b). This result underlines that it is essential to model entire landscapes instead of upscaling conclusions from small-scale studies.

Erosion-induced SOC loss and its partial deposition is most pronounced shortly after land conversion as the topsoil is still rich in SOC. Therefore, results from studies in regions where arable land was established centuries ago (e.g. Dlugoß et al., 2012; Juřicová et al., submitted; Nadeu et al., 2015) might not allow to draw general conclusions for regions where land conversion
405 happened recently. This corroborates the argument from Van Oost and Six (2023) that our understanding of coupled erosion and C turnover processes is strongly biased towards humid/temperate settings, where land conversion mostly occurred centuries ago, while little is known for regions with on-going land conversion often located in tropical regions (Song et al., 2018).

4.3 Tillage-induced soil redistribution and C dynamics

4.3.1 Tillage as the main driver of the erosion-induced C pump

410 Within our study area, tillage erosion was demonstrated to be a critically important process dominating the catchment's C balance and the C sink function induced by soil redistribution. Water erosion cannot be neglected due to extreme events that are responsible for crop losses, high sedimentation rates, and off-site damage (Frielinghaus et al., 1992; Frielinghaus and Schmidt, 1993). However, as illustrated by the historical aerial photograph in Figure 4, tillage-induced soil redistribution in this area is dominating and not only important since the introduction of heavy machinery 70 years ago (Van der Meij et al., 2017;

415 Wilken et al., 2020; Winnige et al., 2003). In addition, tillage is known to further increase the susceptibility of arable soils to water erosion (Lobb et al., 1995) due to its effect on soil microporosity and changes in surface roughness (Poesen and Govers, 1985). The impact of tillage outcompetes soil redistribution by water due to specific conditions in the study area. The farming structures in the post-socialistic study area (large field sizes) perform tillage on a high optimisation level. Within a typical 5-year crop rotation (rapeseed – winter wheat – maize – winter wheat – winter barley) inversion tillage is only applied once

420 between two small-grain cereals, while chisel plough is applied in all other years. The rationale is that chisel ploughing can be applied faster and requires less mechanical force (i.e. kinetic energy) compared to inversion ploughing, which reduces the time effort and fuel consumption, respectively (Dumanski et al., 2006; Helsel, 2007). Furthermore, the hummocky topography of the young morainic study area shows a short summit-foot slope distance that benefits tillage erosion, which does not increase with slope length such as water erosion. This characteristic topography also leads to large depositional areas (41 % of the

425 study area; in comparison to 25 ± 7 % in a global estimate of Van Oost et al., 2007) that favours C burial and sequestration. In addition, there is a low hydrological and sedimentological connectivity to the river system in the study area. Only 5 x 10^{-4} t ha^{-1} of eroded soil are exported by water to the river system, while ca. 20 times more C (0.1 t ha^{-1}) are buried in kettle holes. Even if this limited hydrological connectivity benefits the water-redistribution-induced C sink function, tillage erosion is still dominant as erosive rainfall appears only on a relatively low frequency in this region (Deumlich, 1999; Wilken et al., 2018).

430 #### 4.3.2 Recent developments in tillage-induced soil redistribution

Tillage erosivity partly decreased due to the introduction of pesticides for weed control which reduced the relevance of inversion tillage over the past decades (Lobb et al., 2007). Also in our study area, non-inversion conservation tillage receives more attention and is already applied to 47 % of the cropland area (44 % conventional tillage and 0.06 % no-till; Statistisches Bundesamt (Destatis), 2017). Nevertheless, it needs to be mentioned that conservation tillage focuses on water erosion mitigation,

435 while tillage erosion is not accounted for. A recent study demonstrated that soil tillage by chisel plough leads to substantially more tillage erosion than inversion implements (Öttl et al., 2022). Hence, tillage practices show high spatiotemporal variation, which is fused to a large sensitivity of tillage erosion predictions. The sensitivity is reflected in the erosion pathways, whereby the difference between the C balance of the low and high tillage erosion pathways (C balance R8 – R2) is higher than the difference in the C balance without and with consideration of deep C burial, respectively. Hence, the C balance and corresponding

440 sequestration potential of agricultural soil systems is mainly driven by individual farmers' decisions.

4.4 The way ahead for long-term and large-scale soil redistribution and C dynamics modelling

It is evident that long-term and large-scale simulations are needed to gain understanding of C dynamics, not only for scientific purposes but also to find adapted management strategies to increase soil C sequestration. From our perspective, the implementation of the following three processes would substantially increase the simulation quality of coupled soil redistribution and C
445 turnover models.

4.4.1 Keeping track of topographic change by soil redistribution

The model does not account for topographic change related to soil redistribution (i.e. DEM update). For shorter temporal scales (ca. 50-100 years; e.g. Dlugoß et al., 2012; Nadeu et al., 2015; Wilken et al., 2017b), the topographic change has a limited impact, but for a modelling period of 1000 years, neglecting DEM update affects lateral and vertical C dynamics. In a tillage-
450 erosion dominated study area like the Quillow river catchment, both erosion and deposition processes will be substantially overestimated at individual raster cells (erosion: slope shoulders; deposition: footslopes and field borders). This is due to a constant erosion and deposition pattern, which becomes more relevant towards the end of the simulation period. This means that severe erosion is simulated for a smaller spatial area than it would take place in reality. As a result, at erosional sites substantial dynamic replacement is calculated for a limited number of raster cells and SOC is buried more likely below 1 m
455 at severe depositional sites. The latter is especially critical if the modelled deposition is large enough that deposited C-rich topsoil reaches soil layers below 1 m, where it is assumed that SOC is stable in time (Rumpel and Kögel-Knabner, 2011). Hence, taking the topographic change corresponding to soil redistribution into account would be an important step forward to improve the quality of soil patterns.

4.4.2 Plant feedback on soil degradation

460 Coupling the impact of soil redistribution against plant growth would be a great step towards a better representation of C dynamics in disturbed landscapes. A cornerstone for a landscape to function as a C sink is dynamic replacement of eroded C by fresh biomass C due to the uplift of unsaturated reactive minerals (Doetterl et al., 2016; Harden et al., 1999). However, this calls for constantly high yields and corresponding C input at eroding landscape positions (Doetterl et al., 2016; Van Oost and Six, 2023). As severe long-term soil erosion typically causes declining yields (e.g. Bakker et al., 2004; Den Biggelaar et al.,
465 2001; Herbrich et al., 2018), which was also demonstrated in the study area (Öttl et al., 2021), C input is overestimated at erosional areas. On the other hand, C input is underestimated at depositional areas due to more favourable growing conditions (Öttl et al., 2021; Papiernik et al., 2005; Heckrath et al., 2005), which attenuates overstating the C sink term (Öttl et al., 2021; Quinton et al., 2022).

4.4.3 SOC burial in deeper soil layers (< 1 m)

470 Long-term soil redistribution following land conversion from natural forest to arable land leads to deep burial of SOC (< 1 m; Hoffmann et al., 2013). In our modelling approach the assumptions regarding the stability of SOC buried below 1 m are of

tremendous importance in the range of soil-redistribution induced C fluxes (Figure 7 d). Assuming that all SOC allocated below 1 m would be immediately mineralised, the overall soil-redistribution induced C sink would be only 0.11‰ of mean SOC stocks per year, while it would be 0.66‰ if all SOC stocks would be stabilised. However, long-term modelling of SOC

475 turnover in these deep layers is challenging due to the generally limited knowledge of SOC turnover in deep soils (Rumpel and Kögel-Knabner, 2011) and the fluctuating stagnic soil conditions partly associated with landscape positions where soil is deposited.

5 Conclusions

In this study, the long-term (1000 years) effect of soil redistribution upon C fluxes and SOC stocks was modelled in a study
480 region of 200 km^2 in north-eastern Germany. Different to earlier studies focussing on erosion-induced C fluxes we included the change in SOC stocks following conversion from a natural forest to arable land and accounted for changes in agricultural practises and production over time.

The modelling results from a study area representing ground moraine landscapes as typically found in northern Europe, Asia, and North America indicate that soil redistribution in such regions is resulting in a slight C sink, increasing the landscape-scale
485 SOC stocks by 0.66‰ per year as compared to an area without erosion. This sink function mostly results from tillage-induced soil redistribution, while soil redistribution by water only plays a minor role, which is also quite typical for more continental climatic conditions. Modelling a representative segment of a larger landscape instead of focussing on a small (water) erosion prone area with steeper slopes indicates that the C sink function is less pronounced at this scale. The study also underlines the importance of addressing the soil-redistribution induced C fluxes starting with forest-related SOC stocks before conversion to
490 arable land, because focusing only on the phase of arable soil use alone overestimates the erosion-induced sink function.

Data availability. The long-term precipitation reconstruction (1701-2011) for Europe presented by Pauling et al. (2005) was downloaded from the Climate Explorer (Royal Netherlands Meteorological Institute KNMI / World Meteorological Organization WMO): http://climexp. knmi.nl/selectfield_rapid.cgi?id=someone@somewhere. All other data that support the findings of this study are available from the corresponding author upon request.

495 **Appendix A: Supplementary material**

Table A1. Literature review as basis for the temporal variation of the tillage transport coefficient (k_{til}) values shown in Figure 2 a sorted by period. "Original reference" is the publication where the experiment is described which does not necessarily include the calculated k_{til}-value. "Reference k_{til}-value" is the publication that refers to the original reference but includes the k_{til}-value. Abbreviations: CP = chisel plough, MP = mouldboard plough, TE = tillage implements, D = downslope, UD = alternating up- and downslope, C = contour-parallel, EXP = experiment, SIM = simulation.

Original reference	Reference k_{til}-value	k_{til}-value [kg m⁻¹]	Country	Implement	Period	Slope [%]	Tillage speed [km h⁻¹]	Tillage depth [m]	Bulk density [kg m⁻³]	Tillage direction	Method
Dupin et al. (2009)	Dupin et al. (2009)	9.59	Laos	manual (hoe)	P1	30-90	1.11	0.02	900	C	EXP
Kimaro et al. (2005)	Kimaro et al. (2005)	96	Tanzania	manual (hoe)	P1	31-67	-	0.05	1200	UD	EXP
Su and Zhang (2010)	Su and Zhang (2010)	118	China	manual (hoe)	P1	14-28	-	-	-	UD	Sim
Turkelboom et al. (1999)	Turkelboom et al. (1999)	43.2	Thailand	manual (hoe)	P1	17-82	-	0.09	1100	UD	EXP
Turkelboom et al. (1999)	Turkelboom et al. (1999)	45.1	Thailand	manual (hoe)	P1	17-82	-	0.09	1100	UD	EXP
Turkelboom et al. (1999)	Turkelboom et al. (1999)	48.2	Thailand	manual (hoe)	P1	17-82	-	0.09	1100	UD	EXP
Turkelboom et al. (1999)	Turkelboom et al. (1999)	52.4	Thailand	manual (hoe)	P1	17-82	-	0.09	1100	UD	EXP
Turkelboom et al. (1999)	Van Muysen et al. (2000)	77	Thailand	manual (hoe)	P1	17-82	-	0.09	1100	UD	EXP
Turkelboom et al. (1999)	Turkelboom et al. (1999)	98.7	Thailand	manual (hoe)	P1	17-82	-	0.09	1100	UD	EXP
Wang et al. (2021)	Wang et al. (2021)	108.2	China	manual (hoe)	P1	6-50	-	0.18	1404	D	EXP
Wassmer, 1981	Kimaro et al. (2005)	173	Rwanda	manual (hoe)	P1	60	-	-	-	-	EXP
Zhang et al. (2004a)	Zhang et al. (2004a)	139	China	manual (hoe)	P1	4-47	-	-	-	UD	EXP
Zhang et al. (2004b)	Van Oost et al. (2006)	141	China	manual (hoe)	P1	4-48	-	0.22	1310	UD	EXP
Zhang et al. (2004b)	Zhang et al. (2004b)	153	China	manual (hoe)	P1	4-48	-	-	-	UD	EXP
Zhang et al. (2009)	Zhang et al. (2009)	35	China	manual (hoe)	P1	8-65	-	0.19	1391	C	EXP
Quine et al. (1999c)	Van Oost et al. (2006)	31	China	manual and/or animal-pulled plough	P1, 2	-	-	0.17	1300	C	EXP
Quine et al. (1999c)	Van Oost et al. (2006)	250	China	manual and/or animal-pulled plough	P1, 2	-	-	0.17	1300	UD	SIM
Nyssen et al. (2000)	Nyssen et al. (2000)	68	Ethopia	animal pulled ard plough	P1, 2, 3, 4	3	1.1	0.08	1143	C	SIM

Original reference	Reference k_{til}-value	k_{til}-value [kg m^{-1}]	Country	Implement	Period	Slope [%]	Tillage speed [km h^{-1}]	Tillage depth [m]	Bulk density [kg m^{-3}]	Tillage direction	Method
Nyssen et al. (2000)	Nyssen et al. (2000)	272	Ethopia	animal pulled ard plough	P1, 2, 3, 4	48	1.1	0.08	1143	C	EXP
Dercon et al. (2007)	Dercon et al. (2007)	100	Ecuador	animal pulled ard plough	P1, 2, 3, 4	18-36	-	-	-	C	EXP
Dercon et al. (2007)	Dercon et al. (2007)	300	Ecuador	animal pulled ard plough	P1, 2, 3, 4	18-36	-	-	-	-	EXP
Quine et al. (1999b)	Quine et al. (1999b)	108	China	animal pulled CP	P2, 3, 4	11	-	0.2	1350	-	EXP
Quine et al. (1999b)	Quine et al. (1999b)	113	Zimbabwe	animal pulled CP	P2, 3, 4	6	-	0.2	1350	-	SIM
Barneveld et al. (2009)	Barneveld et al. (2009)	14.3	Syria	animal pulled CP	P2, 3, 4	2-43	-	-	1120	C	EXP
Barneveld et al. (2009)	Barneveld et al. (2009)	34.1	Syria	animal pulled CP	P2, 3, 4	2-43	-	-	1120	UD	EXP
Barneveld et al. (2009)	Barneveld et al. (2009)	47.4	Syria	animal pulled CP	P2, 3, 4	2-43	-	-	1120	UD	EXP
Rymshaw et al. (1997)	Van Oost et al. (2006)	29	Venezuela	animal pulled CP	P2, 3, 4	33-78	-	0.2	1270	C	EXP
Thapa et al. (1999a)	Van Oost et al. (2006)	76	Philippines	animal pulled MP	P2, 3, 4	25-36	-	0.2	730	C	EXP
Thapa et al. (1999b)	Van Oost et al. (2006)	119	Philippines	animal pulled MP	P2, 3, 4	16-22	-	0.2	1000	C	EXP
Thapa et al. (1999b)	Van Oost et al. (2006)	152	Philippines	animal pulled MP	P2, 3, 4	16-22	-	0.2	1000	UD	EXP
Quine et al. (1999b)	Quine et al. (1999b)	243	Lesotho	animal pulled MP (2 animals)	P4	7	-	0.15	1350	-	SIM
Govers et al. (1994)	Govers et al. (1994)	111	Belgium	CP	P5	max. 25	4.5	0.15	1350	-	EXP
Lobb et al. (1999)	Van Muysen et al. (2000)	275	Canada	CP	P5	—	9.6	0.17	1580	-	EXP

Original reference	Reference k_{til}-value	k_{til}-value [kg m^{-1}]	Country	Implement	Period	Slope [%]	Tillage speed [km h^{-1}]	Tillage depth [m]	Bulk density [kg m^{-3}]	Tillage direction	Method
Marques da Silva and Alexandre (2004)	Van Oost et al. (2006)	27	Portugal	CP	P5	14-26	3.4	0.19	1600	-	EXP
Marques da Silva and Alexandre (2004)	Van Oost et al. (2006)	75	Portugal	CP	P5	14-26	3.6	0.11	1600	-	EXP
Poesen et al. (1997)	Van Oost et al. (2006)	282	Spain	CP	P5	2-41	2.3	0.16	1582	-	EXP
Quine et al. (1999a)	Quine et al. (1999a)	657	Spain	CP	P5	-	2.2	0.19	1382	UD	EXP
Tiessen et al. (2007)	Tiessen et al. (2007)	444.66	Canada	CP	P5	2-35	6.9	0.16	1367	-	EXP
Van Muysen and Govers (2002)	Van Muysen and Govers (2002)	123	Belgium	CP	P5	0-15	7.92	0.07	1130	UD	EXP
Van Muysen et al. (2000)	Van Muysen et al. (2000)	225	Belgium	CP	P5	max. 30	5.8	0.15	1560	-	EXP
Van Muysen et al. (2000)	Van Muysen et al. (2000)	545	Belgium	CP	P5	max. 30	7.2	0.2	1250	-	EXP
Mech and Free (1942)	Van Oost et al. (2006)	13	USA	CP (before 1960)	P5	0-20	3.6	0.06	1155	-	-
Mech and Free (1942)	Van Oost et al. (2006)	28	USA	cultivator shovel	P5	10-20	-	0.08	-	UD	-
Marques da Silva and Alexandre (2004)	Marques da Silva and Alexandre (2004)	183	Portugal	harrow	P5	14-26	-	-	-	-	EXP
Mech and Free (1942)	Van Oost et al. (2006)	78	USA	harrow	P5	-	-	0.12	-	UD	-
Tiessen et al. (2010)	Tiessen et al. (2010)	232.93	Costa Rica	harrow	P5	10	4.2	0.28	683	U	EXP
Tiessen et al. (2010)	Tiessen et al. (2010)	468.75	Costa Rica	harrow	P5	10	5.3	0.29	663	UD	EXP
Tiessen et al. (2010)	Tiessen et al. (2010)	788.89	Costa Rica	harrow	P5	10	6.4	0.3	642	D	EXP
De Alba (2001)	Van Oost et al. (2006)	164	Spain	MP	P5	15-35	4.5	0.24	1370	C	-
De Alba (2001)	Van Oost et al. (2006)	204	Spain	MP	P5	15-35	4.5	0.24	1370	UD	-
Gerontidis et al. (2001)	Van Oost et al. (2006)	134	Greece	MP	P5	6-22	4.5	0.2	1420	C	EXP
Gerontidis et al. (2001)	Van Oost et al. (2006)	252	Greece	MP	P5	6-22	4.5	0.3	1420	C	EXP
Gerontidis et al. (2001)	Van Oost et al. (2006)	360	Greece	MP	P5	6-22	4.5	0.4	1420	C	EXP

Original reference	Reference k_{til}-value	k_{til}-value [kg m^{-1}]	Country	Implement	Period	Slope [%]	Tillage speed [km h^{-1}]	Tillage depth [m]	Bulk density [kg m^{-3}]	Tillage direction	Method
Gerontidis et al. (2001)	Van Oost et al. (2006)	383	Greece	MP	P5	6-22	4.5	0.3	1420	UD	EXP
Gerontidis et al. (2001)	Van Oost et al. (2006)	670	Greece	MP	P5	6-22	4.5	0.4	1420	UD	EXP
Govers et al. (1994)	Govers et al. (1994)	234	Belgium	MP	P5	max 25	4.5	0.28	1350	UD	EXP
Heckrath et al. (2006)	Van Oost et al. (2006)	49	Denmark	MP	P5	-	4.9	0.23	1529	C	EXP
Heckrath et al. (2006)	Van Oost et al. (2006)	132	Denmark	MP	P5	-	4	0.26	1490	C	EXP
Heckrath et al. (2006)	Van Oost et al. (2006)	137	Denmark	MP	P5	-	4.1	0.22	1423	S	EXP
Heckrath et al. (2006)	Van Oost et al. (2006)	200	Denmark	MP	P5	-	4.9	0.25	1517	UD	EXP
Heckrath et al. (2006)	Van Oost et al. (2006)	239	Denmark	MP	P5	-	4.1	0.24	1449	S	EXP
Heckrath et al. (2006)	Van Oost et al. (2006)	281	Denmark	MP	P5	-	4.9	0.24	1555	S	EXP
Heckrath et al. (2006)	Van Oost et al. (2006)	335	Denmark	MP	P5	-	6.3	0.26	1507	UD	EXP
Kosmas et al. (2001)	Van Oost et al. (2006)	63	Greece	MP	P5	14-21	4.5	0.18	1598	UD	EXP
Kosmas et al. (2001)	Van Oost et al. (2006)	159.8	Greece	MP	P5	14-21	4.5	0.25	1598	UD	EXP
Lindstrom et al. (1992)	Van Oost et al. (2006)	330	USA	MP	P5	1-14	7.6	0.24	1350	UD	EXP
Lindstrom et al. (1992)	Van Oost et al. (2006)	363	USA	MP	P5	1-14	7.6	0.24	1350	C	EXP
Lobb et al. (1995)	Van Oost et al. (2006)	184	Canada	MP	P5	-	4	0.15	1350	UD	EXP
Lobb et al. (1999)	Van Muysen et al. (2000)	346	Canada	MP	P5	-	6.2	0.23	1350	UD	EXP
Marques da Silva and Alexandre (2004)	Marques da Silva and Alexandre (2004)	770	Portugal	MP	P5	14-26	3.7	0.39	1680	UD	EXP
Montgomery et al. (1999)	Montgomery et al. (1999)	110	USA	MP	P5	7-31	3.6	0.23	1310	C	EXP
Quine and Zhang (2004)	Van Oost et al. (2006)	101	UK	MP	P5	-	5.9	0.21	1374	UD	EXP
Quine and Zhang (2004)	Quine and Zhang (2004)	112	UK	MP	P5	-	5.76	0.22	1420	UD	EXP
Quine et al. (2003)	Van Oost et al. (2006)	324	New Zealand	MP	P5	5-10	7	0.17	1350	UD	EXP
Revel and Guiresse (1995)	Van Oost et al. (2006)	263	France	MP	P5	-	6.5	0.27	1350	UD	-
Tiessen et al. (2007)	Tiessen et al. (2007)	269.77	Canada	MP	P5	2-35	6.3	0.17	1367	-	EXP
Tsara et al. (2001)	Tsara et al. (2001)	793	Greece	MP	P5	5-25	-	0.3	1430	C	EXP

Original reference	Reference k_{til}-value	k_{til}-value [kg m^{-1}]	Country	Implement	Period	Slope [%]	Tillage speed [km h^{-1}]	Tillage depth [m]	Bulk density [kg m^{-3}]	Tillage direction	Method
Van Muysen et al. (1999)	Van Muysen et al. 1999	70	Spain	MP	P5	max. 25	2.7	0.15	1650	UD	EXP
Van Muysen et al. (1999)	Van Muysen et al. 1999	254	Spain	MP	P5	max. 25	1.8	0.33	1070	UD	EXP
Van Muysen and Govers (2002)	Van Muysen and Govers (2002)	169	Belgium	MP	P5	max. 30	5.54	0.21	1561	UD	EXP
Van Muysen and Govers (2002)	Van Muysen and Govers (2002)	224	Belgium	MP	P5	max. 30	5.22	0.25	1498	UD	EXP
Mech and Free (1942)	Van Oost et al. (2006)	24	USA	MP (before 1960)	P5	10-20	3.6	0.08	1155	UD	-
Petersen, 1960	Van Oost et al. (2006)	64	USA	MP (before 1960)	P5	-	3.6	0.16	1239	C	-
Govers et al. (1994)	Van Muysen et al. (2006)	133	Belgium	series of TE	P5	max. 25	-	-	-	UD	EXP
Govers et al. (1994)	Govers et al. (1994)	400	Belgium	series of TE	P5	max. 25	4.5	0.28	1350	UD	EXP
Govers et al. (1994)	Govers et al. (1994)	600	Belgium	series of TE	P5	max. 25	4.5	0.28	1350	UD	EXP
Govers et al. (1996)	Govers et al. (1996)	348	UK	series of TE	P5	5	-	-	-	-	SIM
Govers et al. (1996)	Govers et al. (1996)	397	UK	series of TE	P5	5	-	-	-	-	SIM
Quine et al. (1994)	Quine et al. (1994)	550	Belgium	series of TE	P5	-	-	-	-	UD	-
Van Muysen et al. (2006)	Van Muysen et al. (2006)	781	Belgium	series of TE	P5	0-17	-	-	-	UD	experiment
Wilken et al. (2020)	Wilken et al. (2020)	350	Germany	series of TE	P5	0-18	-	-	-	UD	SIM
Van Muysen et al. (2006)	Van Muysen et al. (2006)	167	Belgium	series of TE	P5	0-17	-	-	-	UD	EXP
Van Oost et al. (2000)	Van Oost et al. (2000)	900	Belgium	series of TE	P5	-	-	-	-	UD	-
Lobb et al. (1999)	Van Muysen et al. (2000)	369	Canada	tandem disc	P5	-	3.02	0.17	1105	UD	EXP

Author contributions. The modelling approach was designed by LKO, PF, and FW. LKO reviewed relevant literature, developed the model, conducted the modelling, processed the data, and designed the figures and tables. Model development was supported by FW and AJ. Data analysis and interpretation were carried out by all authors. The manuscript was drafted by LKO, FW, and PF, while all authors contributed to the discussion and reviewed the final version of the manuscript.

500   *Competing interests.* PF is a member of the editorial board of SOIL. The peer-review process was guided by an independent editor, and the authors have no other competing interests to declare.

Acknowledgements. This work was financed by the DFG project "TilEro" (FI-1216/12-1, SO-302/12-1). We also acknowledge the Landscape Pedology Working Group, Leibniz Centre for Agricultural Landscape Research ZALF e.V. (Müncheberg, Germany) for support and data provision.

References

Amelung, W., Bossio, D., de Vries, W., Kögel-Knabner, I., Lehmann, J., Amundson, R., Bol, R., Collins, C., Lal, R., Leifeld, J., Minasny, B., Pan, G., Paustian, K., Rumpel, C., Sanderman, J., van Groenigen, J. W., Mooney, S., van Wesemael, B., Wander, M., and Chabbi, A.: Towards a global-scale soil climate mitigation strategy, Nat Commun, 11, 5427, 2020.

Anderson, G.: Genesis of hummocky moraine in the Bolmen area, southwestern Sweden, Boreas, 27, 55–67, 1998.

Andrén, O. and Kätterer, T.: ICBM: The introductory carbon balance model for exploration of soil carbon balances, Ecological Applications, 7, 1226–1236, 1997.

Aufdenkampe, A. K., Mayorga, E., Raymond, P. A., Melack, J. M., Doney, S. C., Alin, S. R., Aalto, R. E., and Yoo, K.: Riverine coupling of biogeochemical cycles between land, oceans, and atmosphere, Frontiers in Ecology and the Environment, 9, 53–60, 2011.

Baker, V. R.: Debates - Hypothesis testing in hydrology: Pursuing certainty versus pursuing uberty, Water Resources Research, 53, 1770–1778, 2017.

Bakker, M. M., Govers, G., and Rounsevell, M. D. A.: The crop productivity-erosion relationship: an analysis based on experimental work, Catena, 57, 55–76, 2004.

Barneveld, R. J., Bruggeman, A., Sterk, G., and Turkelboom, F.: Comparison of two methods for quantification of tillage erosion rates in olive orchards of north-west Syria, Soil & Tillage Research, 103, 105–112, 2009.

Batista, P. V. G., Davies, J. A. C., Silva, M. L. N., and Quinton, J. N.: On the evaluation of soil erosion models: Are we doing enough?, Earth-Science Reviews, 197, 2019.

Battin, T. J., Luyssaert, S., Kaplan, L. A., Aufdenkampe, A. K., Richter, A., and Tranvik, L. J.: The boundless carbon cycle, Nature Geoscience, 2, 598–600, 2009.

Bayerl, G.: Geschichte der Landnutzung in der Region Barnim-Uckermark, Materialien der Interdisziplinären Arbeitsgruppe Zukunftsorientierte Nutzung ländlicher Räume - LandInnovation, Nr. 12, 2006.

Behre, K.-E.: Landschaftsgeschichte Norddeutschlands. Umwelt und Siedlung von der Steinzeit bis zur Gegenwart, Wachholtz Verlag, Neumünster, 2008.

Bellamy, P. H., Loveland, P. J., Bradley, R. I., Lark, R. M., and Kirk, G. J.: Carbon losses from all soils across England and Wales 1978-2003, Nature, 437, 245–8, 2005.

Bellassen, V., Angers, D. A., Kowalczewski, T., and Olesen, A.: Soil carbon is the blind spot of European national GHG inventories, Nature Climate Change, 12, 324–331, 2022.

Berhe, A. A., Harden, J. W., Torn, M. S., and Harte, J.: Linking soil organic matter dynamics and erosion-induced terrestrial carbon sequestration at different landform positions, Journal of Geophysical Research: Biogeosciences, 113, 2008.

Bork, H. R., Dalchow, C., Dotterweich, M., Schatz, T., and Schmidtchen, G.: Die Entwicklung der Landschaften Brandenburgs in den vergangenen Jahrtausenden, in: Geschichte der Landwirtschaft in Brandenburg, edited by Klemm, V., Darkow, G., and Bork, H. R., pp. 237–258, Verlag Mezogazda, Budapest, Hungary, 1998.

Bouchoms, S., Wang, Z., Vanacker, V., Doetterl, S., and Van Oost, K.: Modelling long-term soil organic carbon dynamics under the impact of land cover change and soil redistribution, Catena, 151, 63–73, 2017.

De Alba, S.: Modelling the effects of complex topography and patterns of tillage on soil translocation by tillage with mouldboard plough, Journal of Soil and Water Conservation, pp. 335–345, 2001.

Den Biggelaar, C., Lal, R., Wiebe, K., and Breneman, V.: The impact of soil erosion on crop yields in North America, in: Advances in agronomy, edited by Sparks, D. L., vol. 72, pp. 1–52, Academic Press, Massachusetts, 2001.

Dercon, G., Govers, G., Poesen, J., Sánchez, H., Rombaut, K., Vandenbroeck, E., Loaiza, G., and Deckers, J.: Animal-powered tillage erosion assessment in the southern Andes region of Ecuador, Geomorphology, 87, 4–15, 2007.

545 Desmet, P. J. J. and Govers, G.: A GIS procedure for automatically calculating the USLE LS factor on topographically complex landscape units, Journal of Soil and Water Conservation, 51, 427–433, 1996.

Deumlich, D.: Erosive Niederschlage und ihre Eintrittswahrscheinlichkeit im Nordosten Deutschlands. Erosive rainstorms and their probability in Northeast Germany, Meteorologische Zeitschrift, 8, 155–161, 1999.

Deumlich, D., Mioduszewski, W., and Kocmit, A.: Analysis of sediment and nutrient loads due to soil erosion in rivers in the Odra catchment,
550 in: Agricultural effects on ground and surface waters: Research at the edge of science and society, vol. 273, IAHS Publication, Wageningen, the Netherlands, 2002.

Deumlich, D., Schmidt, R., and Sommer, M.: A multiscale soil-landform relationship in the glacial-drift area based on digital terrain analysis and soil attributes, Journal of Plant Nutrition and Soil Science, 173, 843–851, 2010.

DIN ISO: Bodenbeschaffenheit – Ermittlung der Erosionsgefährdung von Böden durch Wasser mit Hilfe der ABAG, 19708:2017-08.

555 Diodato, N., Borrelli, P., Fiener, P., Bellocchi, G., and Romano, N.: Discovering historical rainfall erosivity with a parsimonious approach: A case study in Western Germany, Journal of Hydrology, 544, 1–9, 2017.

Dlugoß, V., Fiener, P., Van Oost, K., and Schneider, K.: Model based analysis of lateral and vertical soil carbon fluxes induced by soil redistribution processes in a small agricultural catchment, Earth Surface Processes and Landforms, 37, 193–208, 2012.

Doetterl, S., Six, J., Van Wesemael, B., and Van Oost, K.: Carbon cycling in eroding landscapes: geomorphic controls on soil organic C pool
560 composition and C stabilization, Global Change Biology, 18, 2218–2232, 2012.

Doetterl, S., Berhe, A. A., Nadeu, E., Wang, Z., Sommer, M., and Fiener, P.: Erosion, deposition and soil carbon: A review of process-level controls, experimental tools and models to address C cycling in dynamic landscapes, Earth-Science Reviews, 154, 102–122, 2016.

Donald, C. M. and Hamblin, J.: The biological yield and harvest index of cereals as agronomic and plant breeding criteria, in: Advances in Agronomy, edited by Brady, N. C., vol. 28, pp. 361–405, Academic Press, 1976.

565 Dumanski, J., Peiretti, R., Benites, J. R., McGarry, D., and Pieri, C.: The paradigm of conservation agriculture, Proceedings of World Association of Soil and Water Conservation, pp. 58–64, 2006.

Dupin, B., de Rouw, A., Phantahvong, K. B., and Valentin, C.: Assessment of tillage erosion rates on steep slopes in northern Laos, Soil & Tillage Research, 103, 119–126, 2009.

DWD Climate Data Center (CDC): Historical hourly station observations of 2 m air temperature and humidity for Germany, version v006,
570 2018.

DWD Climate Data Center (CDC): Historical hourly station observations of precipitation for Germany, version v21.3, 2021.

ESA: Sentinel-2 user handbook, Tech. rep., https://sentinels.copernicus.eu/documents/247904/685211/Sentinel-2_User_Handbook, 2015.

Federal Statistical Office: Statistical yearbook [year] for the Federal Republic of Germany, 1990-2018.

Fiener, P., Dlugoß, V., and Van Oost, K.: Erosion-induced carbon redistribution, burial and mineralisation. Is the episodic nature of erosion
575 processes important?, Catena, 133, 282–292, 2015.

Frielinghaus, M. and Schmidt, R.: On-site and off-site damages by erosion in landscapes of East Germany, in: Farm land erosion in temperate plains environment and hills. Proceedings of the international symposium on farm land erosion, edited by Wicherek, S., Elsevier, Paris, France, 1993.

Frielinghaus, M. and Vahrson, W.-G.: Soil translocation by water erosion from agricultural cropland into wet depressions (morainic kettle

580   holes), Soil & Tillage Research, 46, 23–30, 1998.

Frielinghaus, M., Petelkau, H., and Schmidt, R.: Wassererosion im norddeutschen Jungmoränengebiet, Zeitschrift für Kulturtechnik und
        Landentwicklung, 33, 22–33, 1992.

Gerontidis, D. V. S., Kosmas, C., Detsis, B., Marathianou, M., Zafirious, T., and Tsara, M.: The effect of moldboard plow on tillage erosion
        along a hillslope, Journal of Soil and Water Conservation, 56, 147–152, 2001.

585 Gerwitz, A. and Page, E. R.: An empirical mathematical model to describe plant root systems, Journal of Applied Ecology, 11, 773–781,
        1974.

Govers, G., Vandaele, K., Desmet, P., Poesen, J., and Bunte, K.: The role of tillage in soil redistribution on hillslopes, European journal of
        soil science, 45, 469–478, 1994.

Govers, G., Quine, T. A., Desmet, P. J. J., and Walling, D. E.: The relative contribution of soil tillage and overland flow erosion to soil

590   redistribution on agricultural land, Earth Surface Processes and Landforms, 21, 929–946, 1996.

Harden, J. W., Sharpe, J. M., Parton, W. J., Ojima, D. S., Fries, T. L., Huntington, T. G., and Dabney, S. M.: Dynamic replacement and loss
        of soil carbon on eroding cropland, Global Biogeochemical Cycles, 13, 885–901, 1999.

Heckrath, G., Djurhuus, J., Quine, T. A., Van Oost, K., Govers, G., and Zhang, Y.: Tillage erosion and its effect on soil properties and crop
        yield in Denmark, Journal of Environmental Quality, 34, 312–324, 2005.

595 Heckrath, G., Halekoh, U., Djurhuus, J., and Govers, G.: The effect of tillage direction on soil redistribution by mouldboard ploughing on
        complex slopes, Soil & Tillage Research, 88, 225–241, 2006.

Heinrich, I., Balanzategui, D., Bens, O., Blasch, G., Blume, T., Böttcher, F., Borg, E., Brademann, B., Brauer, A., Conrad, C., Dietze,
        E., Dräger, N., Fiener, P., Gerke, H. H., Güntner, A., Heine, I., Helle, G., Herbrich, M., Harfenmeister, K., Heußner, K.-U., Hohmann,
        C., Itzerott, S., Jurasinski, G., Kaiser, K., Kappler, C., Koebsch, F., Liebner, S., Lischeid, G., Merz, B., Missling, K. D., Morgner, M.,

600   Pinkerneil, S., Plessen, B., Raab, T., Ruhtz, T., Sachs, T., Sommer, M., Spengler, D., Stender, V., Stüve, P., and Wilken, F.: Interdisciplinary
        geo-ecological research across time scales in the Northeast German lowland observatory (TERENO-NE), Vadose Zone Journal, 17, 2018.

Helsel, Z. R.: Fuel requirements and energy savings tips for field operations, Tech. rep., Rutgers Cooperative Extension, 2007.

Herbrich, M., Gerke, H. H., and Sommer, M.: Root development of winter wheat in erosion-affected soils depending on the position in a
        hummocky ground moraine soil landscape, Journal of Plant Nutrition and Soil Science, 181, 147–157, 2018.

605 Herrmann, K.: Pflügen, Säen, Ernten. Landarbeit und Landtechnik in der Geschichte, Deutsches Museum, Rowohlt, 1985.

Hoffmann, T., Schlummer, M., Notebaert, B., Verstraeten, G., and Korup, O.: Carbon burial in soil sediments from Holocene agricultural
        erosion, Central Europe, Global Biogeochemical Cycles, 27, 828–835, 2013.

Intergovernmental Panel on Climate Change: Climate Change and Land: an IPCC Special Report on climate change, desertification, land
        degradation, sustainable land management, food security, and greenhouse gas fluxes in terrestrial ecosystems, Tech. rep., 2019.

610 Juřicová, A., Öttl, L. K., Wilken, F., Chuman, T., Žížala, D., Minařík, R., and Fiener, P.: Tillage erosion as an underestimated driver of carbon
        dynamics, Soil & Tillage Research, submitted.

Kimaro, D. N., Deckers, J. A., Poesen, J., Kilasara, M., and Msanya, B. M.: Short and medium term assessment of tillage erosion in the
        Uluguru Mountains, Tanzania, Soil & Tillage Research, 81, 97–108, 2005.

Kirkels, F. M. S. A., Cammeraat, L. H., and Kuhn, N. J.: The fate of soil organic carbon upon erosion, transport and deposition in agricultural

615   landscapes. A review of different concepts, Geomorphology, 226, 94–105, 2014.

Kosmas, C., Gerontidis, S., Marathianou, M., Detsis, B., Zafiriou, T., Muysen, W. N., Govers, G., Quine, T., and Van Oost, K.: The effects of tillage displaced soil on soil properties and wheat biomass, Soil & Tillage Research, 58, 31–44, 2001.

Koszinski, S., Gerke, H. H., Hierold, W., and Sommer, M.: Geophysical-based modeling of a kettle hole catchment of the morainic soil landscape, Vadose Zone Journal, 12, 2013.

620 Kätterer, T. and Andrén, O.: Long-term agricultural field experiments in Northern Europe: analysis of the influence of management on soil carbon stocks using the ICBM model, Agriculture, Ecosystems & Environment, 72, 165–179, 1999.

Kätterer, T., Reichstein, M., Andrén, O., and Lomander, A.: Temperature dependence of organic matter decomposition: a critical review using literature data analyzed with different models, Biology and Fertility of Soils, 27, 258–262, 1998.

Kuratorium für Technik und Bauwesen in der Landwirtschaft e. V. (KTBL): Faustzahlen für die Landwirtschaft, Darmstadt, Germany, 1951, 625   1970, 1980, 1993, 2005.

Lal, R.: Soil carbon sequestration to mitigate climate change, Geoderma, 123, 1–22, 2004.

Lal, R.: Accelerated soil erosion as a source of atmospheric CO_2, Soil & Tillage Research, 188, 35–40, 2019.

Landesamt für Umwelt, Gesundheit und Verbraucherschutz Brandenburg & Landesvermessung und Geobasisinformation Brandenburg: Digital elevation model with a grid size of 1 m (DEM1) derived from laser scan data, 2012.

630 Le Quéré, C., Andrew, R. M., Canadell, J. G., Sitch, S., Korsbakken, J. I., Peters, G. P., Manning, A. C., Boden, T. A., Tans, P. P., Houghton, R. A., Keeling, R. F., Alin, S., Andrews, O. D., Anthoni, P., Barbero, L., Bopp, L., Chevallier, F., Chini, L. P., Ciais, P., Currie, K., Delire, C., Doney, S. C., Friedlingstein, P., Gkritzalis, T., Harris, I., Hauck, J., Haverd, V., Hoppema, M., Klein Goldewijk, K., Jain, A. K., Kato, E., Körtzinger, A., Landschützer, P., Lefèvre, N., Lenton, A., Lienert, S., Lombardozzi, D., Melton, J. R., Metzl, N., Millero, F., Monteiro, P. M. S., Munro, D. R., Nabel, J. E. M. S., Nakaoka, S.-i., O'Brien, K., Olsen, A., Omar, A. M., Ono, T., Pierrot, D., Poulter, 635   B., Rödenbeck, C., Salisbury, J., Schuster, U., Schwinger, J., Séférian, R., Skjelvan, I., Stocker, B. D., Sutton, A. J., Takahashi, T., Tian, H., Tilbrook, B., van der Laan-Luijkx, I. T., van der Werf, G. R., Viovy, N., Walker, A. P., Wiltshire, A. J., and Zaehle, S.: Global carbon budget 2016, Earth System Science Data, 8, 605–649, 2016.

Li, Y., Zhang, Q. W., Reicosky, D. C., Lindstrom, M. J., Bai, L. Y., and Li, L.: Changes in soil organic carbon induced by tillage and water erosion on a steep cultivated hillslope in the Chinese Loess Plateau from 1898-1954 and 1954-1998, Journal of Geophysical Research, 640   112, 2007.

Lindstrom, M. J., Nelson, W. W., and Schumacher, T. E.: Quantifying tillage erosion rates due to moldboard plowing, Soil & Tillage Research, 24, 243–255, 1992.

Lischeid, G., Balla, D., Dannowski, R., Dietrich, O., Kalettka, T., Merz, C., Schindler, U., and Steidl, J.: Forensic hydrology: what function tells about structure in complex settings, Environmental Earth Sciences, 76, 1–15, 2017.

645 Lobb, D. A., Kachanoski, R. G., and Miller, M. H.: Tillage translocation and tillage erosion on shoulder slope landscape positions measured using ^{137}Cs as a tracer, Canadian Journal of Soil Science, 75, 211–218, 1995.

Lobb, D. A., Kachanoski, R. G., and Miller, M. H.: Tillage translocation and tillage erosion in the complex upland landscapes of southwestern Ontario, Canada, Soil & Tillage Research, 51, 1999.

Lobb, D. A., Huffman, E., and Reicosky, D. C.: Importance of information on tillage practices in the modelling of environmental processes 650   and in the use of environmental indicators, Journal of Environmental Management, 82, 377–87, 2007.

Lüthgens, C., Böse, M., and Preusser, F.: Age of the Pomeranian ice-marginal position in northeastern Germany determined by Optically Stimulated Luminescence (OSL) dating of glaciofluvial sediments, Boreas, 40, 598–615, 2011.

Lugato, E., Smith, P., Borrelli, P., Panagos, P., Ballabio, C., Orgiazzi, A., Fernandez-Ugalde, O., Montanarella, L., and Jones, A.: Soil erosion is unlikely to drive a future carbon sink in Europe, Science Advances, 4, 2018.

655 Marques da Silva, J. R. and Alexandre, C.: Soil carbonation processes as evidence of tillage-induced erosion, Soil & Tillage Research, 78, 217–224, 2004.

Mech, S. J. and Free, G. R.: Movement of soil during tillage operations, Agricultural Engineering, pp. 379–382, 1942.

Minasny, B., Malone, B. P., McBratney, A. B., Angers, D. A., Arrouays, D., Chambers, A., Chaplot, V., Chen, Z.-S., Cheng, K., Das, B. S., Field, D. J., Gimona, A., Hedley, C. B., Hong, S. Y., Mandal, B., Marchant, B. P., Martin, M., McConkey, B. G., Mulder, V. L., O'Rourke,

660 S., Richer-de Forges, A. C., Odeh, I., Padarian, J., Paustian, K., Pan, G., Poggio, L., Savin, I., Stolbovoy, V., Stockmann, U., Sulaeman, Y., Tsui, C.-C., Vågen, T.-G., Van Wesemael, B., and Winowiecki, L.: Soil carbon 4 per mille, Geoderma, 292, 59–86, 2017.

Montgomery, D. R.: Soil erosion and agricultural sustainability, Proceedings of the National Academy of Sciences of the United States of America, 104, 13 268–13 272, 2007.

Montgomery, J. A., McCool, D. K., Busacca, A. J., and Frazier, B. E.: Quantifying tillage translocation and deposition rates due to moldboard

665 plowing in the Palouse region of the Pacific Northwest, USA, Soil & Tillage Research, 51, 175–187, 1999.

Nadeu, E., Gobin, A., Fiener, P., Van Wesemael, B., and Van Oost, K.: Modelling the impact of agricultural management on soil carbon stocks at the regional scale: the role of lateral fluxes, Global Change Biology, 21, 3181–92, 2015.

Naipal, V., Ciais, P., Wang, Y., Lauerwald, R., Guenet, B., and Van Oost, K.: Global soil organic carbon removal by water erosion under climate change and land use change during AD 1850-2005, Biogeosciences, 15, 4459–4480, 2018.

670 Nash, J. E. and Sutcliffe, J. V.: River flow forecasting through conceptual models. Part I: A discussion of principles, Journal of Hydrology, 10, 282–290, 1970.

Nyssen, J., Poesen, J., Haile, M., Moeyersons, J., and Deckers, J.: Tillage erosion on slopes with soil conservation structures in the Ethiopian highlands, Soil & Tillage Research, 57, 115–127, 2000.

Papiernik, S. K., Lindstrom, M. J., Schumacher, J. A., Farenhorst, A., Stephens, K. D., Schumacher, T. E., and Lobb, D. A.: Variation in soil

675 properties and crop yield across an eroded prairie landscape, Journal of Soil and Water Conservation, 60, 388–395, 2005.

Pauling, A., Luterbacher, J., Casty, C., and Wanner, H.: Five hundred years of gridded high-resolution precipitation reconstructions over Europe and the connection to large-scale circulation, Climate Dynamics, 26, 387–405, 2005.

Pianosi, F., Beven, K., Freer, J., Hall, J. W., Rougier, J., Stephenson, D. B., and Wagener, T.: Sensitivity analysis of environmental models: A systematic review with practical workflow, Environmental Modelling & Software, 79, 214–232, 2016.

680 Poesen, J. and Govers, G.: A field-scale study on surface sealing and compaction on loam and sandy loam soils. Part II. Impact of soil surface sealing and compaction on water erosion processes, in: Assessment of soil surface sealing and crusting, edited by Callebaut, F., Gabriels, D., and De Broodt, M., pp. 183–193, Ghent, Belgium, 1985.

Poesen, J., Van Wesemael, B., Govers, G., Martinez-Fernandez, J., Desmet, P., Vandaele, K., Quine, T., and Degraer, G.: Patterns of rock fragment cover generated by tillage erosion, Geomorphology, 18, 183–197, 1997.

685 Quine, T. A. and Zhang, Y.: Re-defining tillage erosion: quantifying intensity–direction relationships for complex terrain. 2. Revised mould-board erosion model, Soil Use and Management, 20, 124–132, 2004.

Quine, T. A., Desmet, P. J. J., Govers, G., Vandaele, K., and Walling, D. E.: A comparison of the roles of tillage and water erosion in landform development and sediment export on agricultural land near Leuven, Belgium, Variability in Stream Erosion and Sediment Transport, 224, 77–86, 1994.

690   Quine, T. A., Govers, G., Poesen, J., Walling, D., Van Wesemael, B., and Martinez-Fernandez, J.: Fine-earth translocation by tillage in stony soils in the Guadalentin, south-east Spain: an investigation using caesium-134, Soil & Tillage Research, 51, 279–301, 1999a.

Quine, T. A., Walling, D. E., Chakela, Q. K., Mandiringana, O. T., and Zhang, X.: Rates and patterns of tillage and water erosion on terraces and contour strips: evidence from caesium-137 measurements, Catena, 36, 115–142, 1999b.

Quine, T. A., Walling, D. E., and Zhang, X.: Tillage erosion, water erosion and soil quality on cultivated terraces near Xifeng in the loess

695   plateau, China, Land Degradation & Development, 10, 251–274, 1999c.

Quine, T. A., Basher, L. R., and Nicholas, A. P.: Tillage erosion intensity in the South Canterbury Downlands, New Zealand, Australian Journal of Soil Research, 41, 789–807, 2003.

Quinton, J. N., Öttl, L. K., and Fiener, P.: Tillage exacerbates the vulnerability of cereal crops to drought, Nature Food, 3, 472–479, 2022.

Renard, K. G., Foster, G. R., Weesies, G. A., McCool, D. K., and Yoder, D. C.: Predictig soil erosion by water: A guide to conservation

700   planning with the Revised Universal Soil Loss Equation (RUSLE), Agriculture Handbook 703, 1997.

Revel, J. C. and Guiresse, M.: Erosion due to cultivation of calcareous clay soils on the hillsides of south west France. I. Effect of former farming practices, Soil & Tillage Research, 35, 147–155, 1995.

Ritchie, H. and Roser, M.: Crop yields, https://ourworldindata.org/crop-yields, 2013.

Rosenbloom, N. A., Doney, S. C., and Schimel, D. S.: Geomorphic evolution of soil texture and organic matter in eroding landscapes, Global

705   Biogeochemical Cycles, 15, 365–381, 2001.

Rösener, W.: Arbeitsgerät, Bodennutzung und agrarwirtschaftlicher Fortschritt, in: Bauern im Mittelalter, edited by Rösener, W., pp. 118–133, C. H. Beck'sche Verlagsbuchhandlung, Munich, 1985.

Rumpel, C. and Kögel-Knabner, I.: Deep soil organic matter - a key but poorly understood component of terrestrial C cycle, Plant and Soil, 338, 143–158, 2011.

710   Rymshaw, E., Walter, M. F., and Van Wambeke, A.: Processes of soil movement on steep cultivated hill slopes in the Venezuelan Andes, Soil & Tillage Research, 44, 265–272, 1997.

Sanderman, J., Hengl, T., and Fiske, G. J.: Soil carbon debt of 12,000 years of human land use, Proceedings of the National Academy of Sciences, 114, 9575–9580, 2017.

Schwertmann, U., Vogl, W., and Kainz, M.: Bodenerosion durch Wasser. Vorhersage des Bodenabtrags und Bewertung von Gegenmaßnah-

715   men., Ulmer Verlag, Stuttgart, Germany, 1987.

Sommer, M., Gerke, H. H., and Deumlich, D.: Modelling soil landscape genesis. A "time split" approach for hummocky agricultural landscapes, Geoderma, 145, 480–493, 2008.

Sommer, M., Hoffmann, M., Gerke, H. H., and Meier, K.: Multiyear soil, plant, weather and treatment data from an erosion-affected soil landscape in the Uckermark region, 2020.

720   Song, X. P., Hansen, M. C., Stehman, S. V., Potapov, P. V., Tyukavina, A., Vermote, E. F., and Townshend, J. R.: Global land change from 1982 to 2016, Nature, 560, 639–643, 2018.

Staatliche Zentralverwaltung für Statistik: Statistisches Jahrbuch der Deutschen Demokratischen Republik [year], 1956-1990.

Stallard, R. F.: Terrestrial sedimentation and the carbon cycle: Coupling weathering and erosion to carbon burial, Global Biogeochemical Cycles, 12, 231–257, 1998.

725   Statistisches Bundesamt (Destatis): Land- und Forstwirtschaft, Fischerei. Bodenbearbeitung, Erosionsschutz, Fruchtwechsel / Agrarstruktur-erhebung. 2016, 2017.

Su, Z. A. and Zhang, J. H.: Effects of tillage erosion on soil redistribution in a purple soil with steep sloping terraces, 2010.

Thapa, B. B., Cassel, D. K., and Garrity, D. P.: Assessment of tillage erosion rates on steepland Oxisols in the humid tropics using granite rocks, Soil & Tillage Research, 51, 233–243, 1999a.

730 Thapa, B. B., Cassel, D. K., and Garrity, D. P.: Ridge tillage and contour natural grass barrier strips reduce tillage erosion, Soil & Tillage Research, 51, 341–356, 1999b.

Tiessen, K. H. D., Mehuys, G. R., Lobb, D. A., and Rees, H. W.: Tillage erosion within potato production systems in Atlantic Canada: I. Measurement of tillage translocation by implements used in seedbed preparation, Soil & Tillage Research, 95, 308–319, 2007.

Tiessen, K. H. D., Sancho, F. M., Lobb, D. A., and Mehuys, G. R.: Assessment of tillage translocation and erosion by the disk plow on
735 steepland Andisols in Costa Rica, Journal of Soil and Water Conservation, 65, 316–328, 2010.

Tsara, M., Gerontidis, S., Marathianou, M., and Kosmas, C.: The long-term effect of tillage on soil displacement of hilly areas used for growing wheat in Greece, Soil Use and Management, 17, 113–120, 2001.

Öttl, L. K., Wilken, F., Auerswald, K., Sommer, M., Wehrhan, M., and Fiener, P.: Tillage erosion as an important driver of in-field biomass patterns in an intensively used hummocky landscape, Land Degradation & Development, 32, 3077–3091, 2021.

740 Öttl, L. K., Wilken, F., Hupfer, A., Sommer, M., and Fiener, P.: Non-inversion conservation tillage as an underestimated driver of tillage erosion, Scientific Reports, 12, 2022.

Tum, M. and Günther, K. P.: Validating modelled NPP using statistical yield data, Biomass and Bioenergy, 35, 4665–4674, 2011.

Turkelboom, F., Poesen, J., Ohler, I., and Ongprasert, S.: Reassessment of tillage erosion rates by manual tillage on steep slopes in northern Thailand, Soil & Tillage Research, 51, 245–259, 1999.

745 United Nations Framework Convention on Climate Change: Kyoto Protocol to the United Nations Framework Convention on Climate Change, Tech. rep., 1998.

Van der Meij, W. M., Temme, A. J. A. M., Wallinga, J., Hierold, W., and Sommer, M.: Topography reconstruction of eroding landscapes. A case study from a hummocky ground moraine (CarboZALF-D), Geomorphology, 295, 758–772, 2017.

Van der Meij, W. M., Reimann, T., Vornehm, V. K., Temme, A. J. A. M., Wallinga, J., Beek, R., and Sommer, M.: Reconstructing rates and
750 patterns of colluvial soil redistribution in agrarian (hummocky) landscapes, Earth Surface Processes and Landforms, 2019.

Van Muysen, W. and Govers, G.: Soil displacement and tillage erosion during secondary tillage operations: the case of rotary harrow and seeding equipment, Soil & Tillage Research, 65, 185–191, 2002.

Van Muysen, W., Govers, G., Bergkamp, G., Roxo, M., and Poesen, J.: Measurement and modelling of the effects of initial soil conditions and slope gradient on soil translocation by tillage, Soil & Tillage Research, 51, 303–316, 1999.

755 Van Muysen, W., Govers, G., Van Oost, K., and Van Rompaey, A.: The effect of tillage depth, tillage speed, and soil condition on chisel tillage erosivity, Journal of Soil and Water Conservation, 55, 355–364, 2000.

Van Muysen, W., Van Oost, K., and Govers, G.: Soil translocation resulting from multiple passes of tillage under normal field operating conditions, Soil & Tillage Research, 87, 218–230, 2006.

Van Oost, K. and Six, J.: Reconciling the paradox of soil organic carbon erosion by water, Biogeosciences, 20, 635–646, 2023.

760 Van Oost, K., Govers, G., and Desmet, P.: Evaluating the effects of changes in landscape structure on soil erosion by water and tillage, Landscape Ecology, 15, 577–589, 2000.

Van Oost, K., Govers, G., and Van Muysen, W.: A process-based conversion model for caesium-137 derived erosion rates on agricultural land: an integrated spatial approach, Earth Surface Processes and Landforms, 28, 187–207, 2003.

Van Oost, K., Govers, G., Quine, T. A., Heckrath, G., Olesen, J. E., De Gryze, S., and Merckx, R.: Landscape-scale modeling of carbon
765 cycling under the impact of soil redistribution: The role of tillage erosion, Global Biogeochemical Cycles, 19, 2005.

Van Oost, K., Govers, G., De Alba, S., and Quine, T. A.: Tillage erosion: A review of controlling factors and implications for soil quality, Progress in Physical Geography, 30, 443–466, 2006.

Van Oost, K., Quine, T. A., Govers, G., De Gryze, S., Six, J., Harden, J. W., Ritchie, J. C., McCarty, G. W., Heckrath, G., Kosmas, C., Giraldez, J. V., Marques da Silva, J. R., and Merckx, R.: The impact of agricultural soil erosion on the global carbon cycle, Science, 318, 626–629, 2007.

Verch, G.: Longterm effects of different mineral and organic fertilizer and soil cultivation on the yield in a crop rotation (Northeast Germany), 2020.

Volkert, W.: Dreifelderwirtschaft, in: Adel bis Zunft. Ein Lexikon des Mittelalters, edited by Volkert, W., p. 49, C. H. Beck'sche Verlagsbuchhandlung, Munich, 1991.

Wang, Y., Zhang, Z., Zhang, J., Liang, X., Liu, X., and Zeng, Y.: Effect of surface rills on soil redistribution by tillage erosion on a steep hillslope, Geomorphology, 380, 2021.

Wang, Z., Hoffmann, T., Six, J., Kaplan, J. O., Govers, G., Doetterl, S., and Van Oost, K.: Human-induced erosion has offset one-third of carbon emissions from land cover change, Nature Climate Change, 7, 345–349, 2017.

Wehrhan, M. and Sommer, M.: A parsimonious approach to estimate soil organic carbon applying unmanned aerial system (UAS) multispectral imagery and the topographic position index in a heterogeneous soil landscape, Remote Sensing, 13, 2021.

Wilken, F., Fiener, P., and Van Oost, K.: Modelling a century of soil redistribution processes and carbon delivery from small watersheds using a multi-class sediment transport model, Earth Surface Dynamics, 5, 113–124, 2017a.

Wilken, F., Sommer, M., Van Oost, K., Bens, O., and Fiener, P.: Process-oriented modelling to identify main drivers of erosion-induced carbon fluxes, Soil, 3, 83–94, 2017b.

Wilken, F., Baur, M., Sommer, M., Deumlich, D., Bens, O., and Fiener, P.: Uncertainties in rainfall kinetic energy-intensity relations for soil erosion modelling, Catena, 171, 234–244, 2018.

Wilken, F., Ketterer, M., Koszinski, S., Sommer, M., and Fiener, P.: Understanding the role of water and tillage erosion from $^{239+240}$Pu tracer measurements using inverse modelling, Soil, 6, 549–564, 2020.

Winnige, B., Frielinghaus, M., and Li, Y.: Bedeutung der Bearbeitungserosion im Jungmoränengebiet, in: Mitteilungen der Deutschen Bodenkundlichen Gesellschaft, vol. 101, pp. 93–94, 2003.

Zhang, J., Lobb, D. A., Li, Y., and Liu, G. C.: Assessment of tillage translocation and tillage erosion by hoeing on the steep land in hilly areas of Sichuan, China, Soil & Tillage Research, 75, 99–107, 2004a.

Zhang, J. H., Frielinghaus, M., Tian, G., and Lobb, D. A.: Ridge and contour tillage effects on soil erosion from steep hillslopes in the Sichuan Basin, China, Journal of Soil and Water Conservation, 59, 277–284, 2004b.

Zhang, J. H., Su, Z. A., and Nie, X. J.: An investigation of soil translocation and erosion by conservation hoeing tillage on steep lands using a magnetic tracer, Soil & Tillage Research, 105, 177–183, 2009.